Int J Pept Res Ther
DOI 10.1007/s10989-015-9509-1

Synthesis of Novel Protected N_α(ω-Drug) Amino Acid Building Units for Facile Preparation of Anticancer Drug-Conjugates

Y. Gilad[1,2] · S. Waintraub[2] · A. Albeck[2] · G. Gellerman[1]

Accepted: 29 December 2015

Abstract We report about the preparation of novel protected N_α(ω-drug) amino acid building units and their straightforward incorporation in solid phase synthesis for the preparation of peptide-drug conjugates. These building units were synthesized applying various coupling methods between anticancer drugs and the side chains of different N_α protected amino acids. Subsequent incorporation of these amino acid-drug motifs into linear and cyclic integrin RGD and NGR containing ligands enabled a non-linear/divergent synthetic pathway of medicinally potential peptide-drug conjugates. The synthetic routes reported in this work are both general and applicable, and significantly expand the scope of the conjugation capabilities for peptide drug conjugates. For the preliminary in vitro evaluation of the novel peptide-drug conjugates reported herein, selective cytotoxicity of two representatives—one linear and one cyclic RGD—camptothecin conjugates were evaluated on $\alpha_v\beta_3$ integrin overexpressed cancer cell lines.

Graphical Abstract

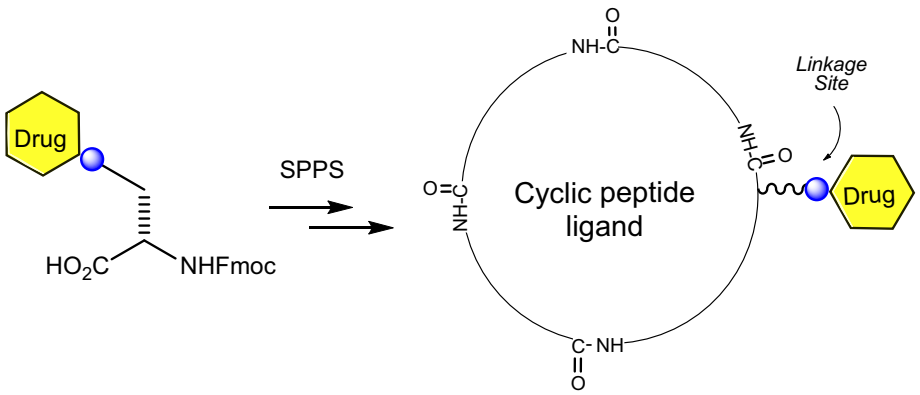

Keywords Amino acid building units · Anticancer drugs · Solid phase synthesis · Peptide drug conjugates

Abbreviations

AABU	Amino acid building units
BU	Building unit
DCC	N,N′-dicyclohexylcarbodiimide
DCM	Dichloromethane
DIPEA	N,N′-diisopropylethylamine
DMF	Dimethylformamide

Electronic supplementary material The online version of this article (doi:10.1007/s10989-015-9509-1) contains supplementary material, which is available to authorized users.

✉ G. Gellerman
garyg@ariel.ac.il

[1] Department of Biological Chemistry, Ariel University, 40700 Ariel, Israel

[2] The Julius Spokojny Bioorganic Chemistry Laboratory, Department of Chemistry, Bar Ilan University, 52900 Ramat Gan, Israel

Published online: 08 January 2016

EDC	1-Ethyl-3-(3-Dimethylaminopropyl) Carbodiimide Hydrochloride
Fmoc	N-(9-Fluorenylmethoxycarbonyl)
IBCF	Isobutyl Chloroformate
NE	Not evaluated
PNFC	*para*-Nitro phenyl chloroformate
SPPS	Solid phase peptide synthesis
TFA	Trifluoroacetic acid
THF	Tetrahydrofuran
TMS	Trimethylsilyl

Introduction

Significant research efforts have been invested in recent years in the development of peptide therapeutics. Continuing progress in synthetic peptide chemistry over the ensuing years has largely solved many of the problems to the extent that the field is flourishing today (Bellmann-Sickert and Beck-Sickinger 2010). Recent surveys show that over 50 peptide drugs have been approved for clinical use. Another several hundred peptides are in various stages of clinical assessment (Firer and Gellerman 2012). This data gives a strong impetus to using peptides as drug carriers for a variety of medicinal applications and especially for cancer therapy.

Angiogenesis and metastasis are cell adhesion processes mediated by heterodimeric transmembrane glycoprotein receptors of the integrin family (Haubner et al. 1997; Ruoslahti 1996). Tumor-induced angiogenesis is a consequence of ligation by extracellular matrix proteins to the $\alpha_v\beta_3$ integrin (Plow et al. 2000), which is highly expressed on many tumor cells (Lafrenie et al. 1994). A common binding motif in these matrix proteins is the amino acid sequence arginine-glycine-aspartic acid (RGD). Another binding motif with affinity to tumor vasculature is CD13 receptor ligand, asparagine-glycine-arginine (NGR) (Arap et al. 1998; Colombo et al. 2002; Pasqualini et al. 2000; Soudy et al. 2012; van Hensbergen et al. 2002). Blocking tumor-induced angiogenesis by inhibition of the $\alpha_v\beta_3$ integrin is now a major target for cancer chemotherapy (Cheng et al. 2014; Goodman and Picard 2012), and many RGD-containing peptides have been evaluated as antagonists of integrins (Danhier et al. 2012).

We are also investigating $\alpha_v\beta_3$ integrin peptidic antagonists as delivery vehicles for highly cytotoxic warheads, while focusing on the important question of appropriate carrier-linker-drug design and synthesis of peptide drug conjugates (PDCs). The site of conjugation between the peptide and the drug molecule can have a profound effect on maintaining peptide binding affinity, drug release, activity and conjugate stability (Gilad et al. 2014). However, exact knowledge of the peptide sequence and the amino acids responsible for maintaining of high binding affinity often allows a higher degree of flexibility in the design of linker length, its composition and conjugation chemistry to the drug. Peptide conjugation can then include a wide range of functional groups encompassing amides, carboxylic acid esters, hydrazones, thioethers and carbamates (Majumdar and Siahaan 2012).

Based on the above, we decided to develop an efficient synthesis of premade ready-to-use Nα-Fmoc protected amino acid building units that bear anticancer drugs through various biodegradable bonds, for incorporation in parallel solid phase synthesis of peptide-drug conjugates.

The rationale behind the concept presented herein is based on the following: (1) premade Nα-Fmoc protected AA-drug building units can be incorporated into peptide sequence using the convenient standard Fmoc chemistry protocol, enabling efficient high throughput parallel divergent synthesis (Friligou et al. 2013) of linear and cyclic peptide-drug conjugates; (2) Fmoc–AA(drug)–OH building units containing biodegradable moieties: ester, carbamate and amide, which potentiate enzymatic cleavage from the conjugate in vivo (Vig et al. 2013); (3) The drug release profile will depend on the nature of the linker (AA side chain), position in the peptide sequence, linking moiety and the drug itself, as we have already show in our previous study (Gilad et al. 2014). Consequently, drugs can be linked to the peptide carrier through the appropriate building unit at various positions in the peptide sequence for fast evaluation of positioning and drug release parameters.

By optimizing these parameters in the design of peptide carrier-drug conjugates we hope to release the payload specifically in the target cancer cells and thereby avoid exposure of benign tissues to the cytotoxic treatment (Cohen et al. 2007). We anticipate that the utilization of the Fmoc–AA(drug) building units can be integrated into the rational design and application of targeted drug delivery strategies and ultimately expand the scope of the conjugation capabilities for PDCs in general. Preparation of extended repertoire of Fmoc–AA(drug)–OH, their incorporation into other peptide carriers and investigation of targeted therapeutic properties is an ongoing process in our lab.

Results and Discussion

Synthesis of N_α(ω-Drug) Amino Acid (AA) Building Units (BUs)

In several recent reports we discussed the synthesis of functional amino acid building blocks for peptidomimetic assembly and as scaffolds bearing various bioactive modalities. (Gellerman et al. 2001). Kriek et al. reported on uridylylated tyrosine and serine building blocks for stepwise

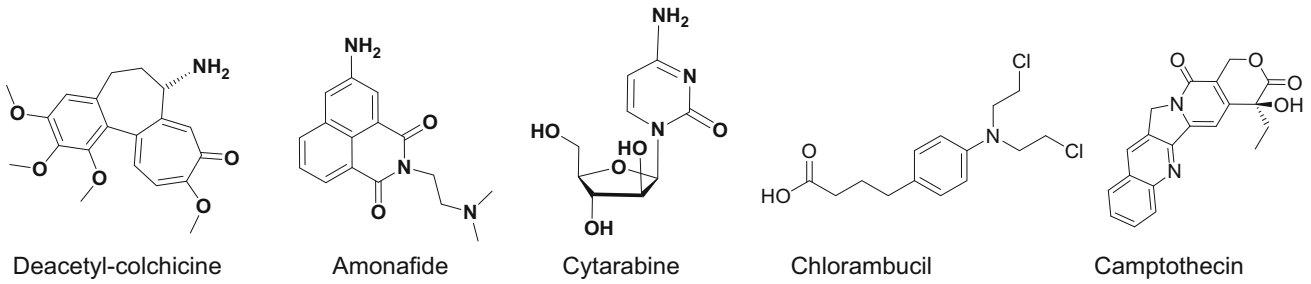

Fig. 1 Drugs that used for the preparation of the AABUs

solid phase synthesis of viral genome-linked peptides (Kriek et al. 2003) using tritylation or allylation of metal-salt Fmoc–AA–OH for regioselective esterification of free carboxylic acids. The following functionalization of the side chain and consequent deprotection yielded the desired building blocks. We decided to implement the same strategy, but with several modifications, for preparing an extended repertoire of Fmoc–AA(drug)–OH building units. The drugs that were selected to assess the feasibility of this mission were five—mechanistically distinguished and with different chemical functions: (1) old DNA mustard alkylating drug—chlorambucil (CLB) with free carboxylic group; (2) topoisomerase II intercalating agent—amonafide (AM) with free aromatic NH_2; (3) topoisomerase I inhibitor camptothecin (CPT), with tertiary OH; (4) Microtubulin poison—colchicine, which after deacetylation (Bagnato et al. 2004) revealed a primary amine; (5) cytarabine—antimetabolite which is mainly used (alone or together with other drugs) in treatment of cancers of white blood cells—with the cytosine aromatic amine. Structures of the mentioned drugs are shown in Fig. 1.

First, Fmoc amino acids that possess hydroxyl functionality at their side chain (Ser, Thr and Tyr) were subjected to the tritylation with 2-chlorotrityl chloride using optimized conditions (as described in the experimental section) leading to the intermediate esters **2a–c** (Scheme 1). Then, **2a–c** were directly reacted with active

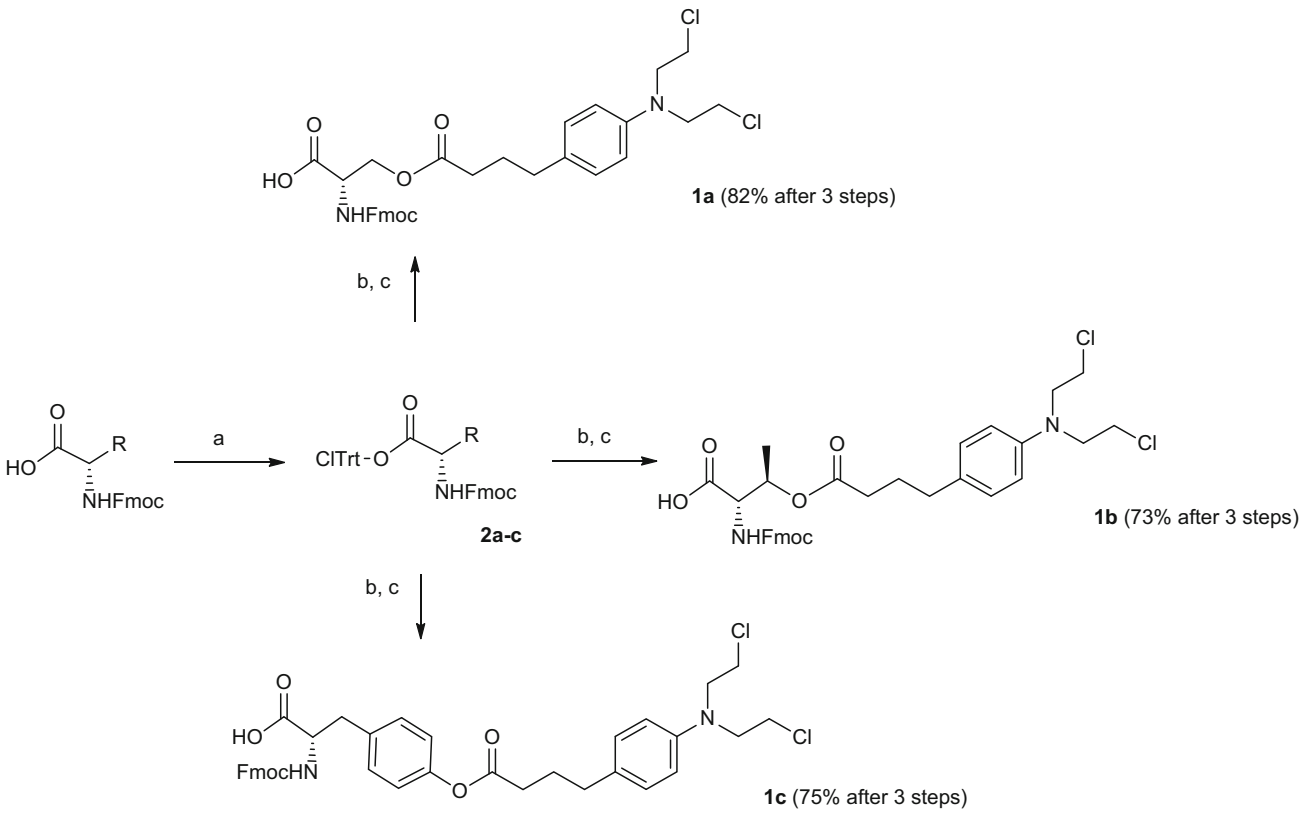

Scheme 1 Synthesis of ester BUs **1a–c**: CLB-Ser, -Thr and -Tyr AA BUs. *a* 2-ClTrt-Cl, DIPA, 2 h, rt; *b* Chlorambucil, HOBt, DCC, DMAP, overnight, rt; *c* 3 % TFA/DCM

ester of CLB, followed by acidic hydrolysis to recover—after purification—the corresponding Fmoc–Ser(CLB)–OH **1a**, Fmoc–Thr(CLB)–OH **1b** and Fmoc–Tyr(CLB)–OH **1c** building units in good yields. Notably, the DNA alkylating drug CLB is linked to the side chains of these BUs through different biodegradable esters: namely, in Ser BU **1a** through a primary alkyl ester, in Thr BU **1b** through a secondary alkyl ester and in Tyr BU **1c** through a phenolic ester. Such structurally controllable linkage of CLB will define a more adequate and adjustable release profile of the drug from the peptide conjugate (Goldshaid et al. 2010).

At this stage we moved to the two-step synthesis of Fmoc–Asp/Glu(drug)–OH amide-BUs **3a–f**, starting from commercially available Fmoc–AA mono esters (Scheme 2). At the beginning, N_{α}-Fmoc-protected Asp or Glu bearing orthogonal protecting group on their alpha carboxylic group, were subjected to coupling reaction with AM, cytarabine (Cyt) and deacetylated colchicine using either standard peptide coupling conditions, utilizing PyBop coupling reagent, or via asymmetric anhydride (Manfredini et al. 2000) resulting intermediates **4a–l** (for yields see Table 1 in Supplementary Information). The purpose of this study was to compare coupling conditions for affording optimized AA drug coupling protocol. After their isolation, the C-terminal protected intermediates were subjected to an appropriate deprotection conditions, leading to the desired BUs **3a–f** (for yields see Table 2 in Supplementary Information). Overall, asymmetric anhydride *i*-butyl chloroformate (IBCF) coupling method using Fmoc–AA–OtBu starting materials was found as more effective.

Next, commercially available Fmoc–Lys(Boc)–OH was employed in the two-step synthesis of Fmoc–Lys(CPT)–OH building block **5** (Scheme 3), in which CPT is linked to the side chain amine through a carbamate bond.

Encouraged by the facile and successful synthesis of the above building blocks, we decided to use them for a preparation of peptide-drug conjugates. Therefore, standard Fmoc SPPS, including a step of BU incorporation was utilized. This resulted in a serial of four cyclic and one linear RGD-containing peptide-drug conjugates, as described below.

Synthesis of a Linear RGD-NGR Peptide-Drug Conjugate

First we demonstrated the ease and effectiveness of incorporation of our building unit into a linear peptide. For this purpose we chose as a model two different tumor vessels targeting motifs—RGD, (integrin $\alpha_v\beta_3$ targeting moiety) (Arap et al. 1998; Chen and Chen 2011), and NGR (CD 13 targeting moiety) (Pasqualini et al. 2000)—which are both routinely employed for developing tumor vasculature targeted delivery systems and imaging agents in various peptide conjugates (Corti et al. 2008; Danhier et al. 2012; Ruoslahti 2002). Such an approach of covalent fusion of two distinct targeting motifs—addressing different receptors of the tumor vasculature—may increase the targeting effectivity of this kind of delivery systems.

Moreover, the NGR motif resembles the $\alpha_v\beta_3$ ligand—RGD, and it is well documented that under physiological conditions a spontaneous rearrangement turns NGR into

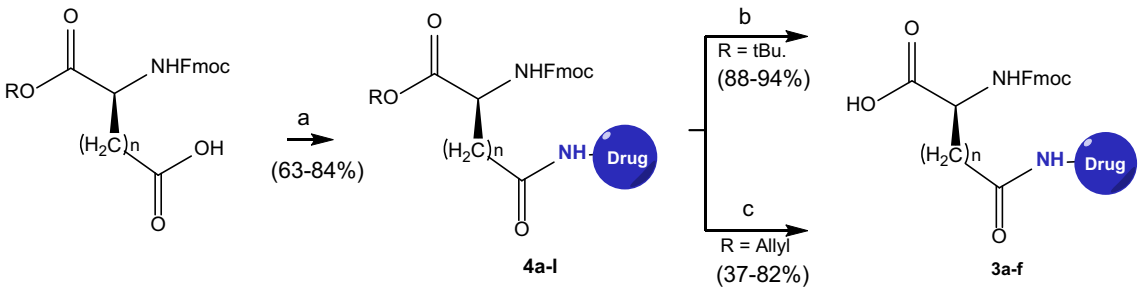

4a, R = tBu n = 1 Drug = Deacetyl colchicine
4b, R = tBu n = 2 Drug = Deacetyl colchicine
4c, R = tBu n = 1 Drug = Amonafide
4d, R = tBu n = 2 Drug = Amonafide
4e, R = tBu n = 1 Drug = Cytarabine
4f, R = tBu n = 2 Drug = Cytarabine
4g, R = Allyl n = 1 Drug = Deacetyl colchicine
4h, R = Allyl n = 2 Drug = Deacetyl colchicine
4i, R = Allyl n = 1 Drug = Amonafide
4j, R = Allyl n = 2 Drug = Amonafide
4k, R = Allyl n = 1 Drug = Cytarabine
4l, R = Allyl n = 2 Drug = Cytarabine

3a, n = 1 Drug = Deacetyl colchicine
3b, n = 2 Drug = Deacetyl colchicine
3c, n = 1 Drug = Amonafide
3d, n = 2 Drug = Amonafide
3e, n = 1 Drug = Cytarabine
3f, n = 2 Drug = Cytarabine

Scheme 2 Synthesis of amide BUs **3a–f**: amonafide/cytarabine/deacetyl colchicine, -Asp, -Glu AA BU. *a* Drug, PyBop, HOBt, DIPA/DMF or Drug, IBCF, TEA; *b* TFA/DCM; *c* Pd(PPh3)4, DMBA/DCM, 4 h, rt

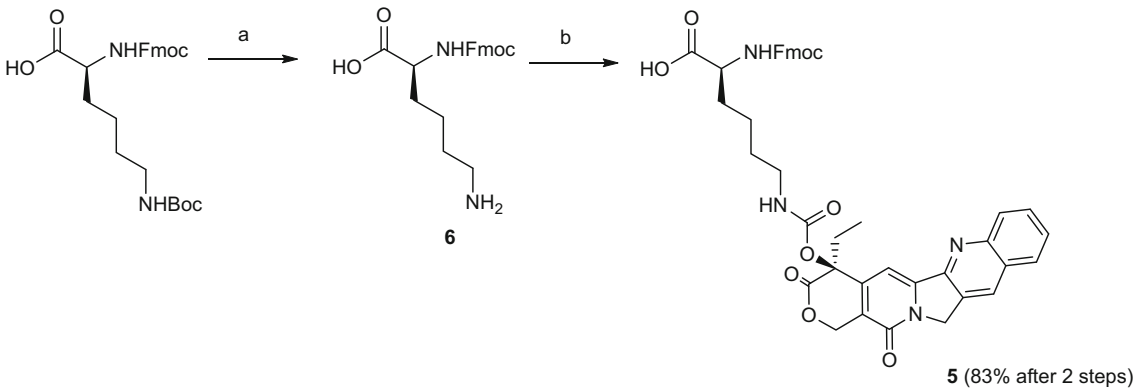

Scheme 3 Synthesis of the carbamate AABU **5**. *a* 90 % TFA/DCM, 90 min, rt; *b* i. CPT, p-nitrophenyl chloroformate, DMF. ii. DIPA/DMF

*iso*DGR (Corti and Curnis 2011; Reissner and Aswad 2003; Robinson et al. 2004), which also exhibits relatively high binding affinity to the $\alpha_v\beta_3$ integrin (Curnis et al. 2006).

Therefore, for demonstrating the applicability of our BUs as connecting elements between two distinct peptidic sequences, we decided to construct the linear peptide **7**, where RGD and NGR sequences are connected through Fmoc–Lys(CPT)–OH building unit **5** (Scheme 4). A linear hepta-peptide-drug conjugate was resulted, containing two different targeting moieties with Topoisomerase I intercalating agent CPT linked through the biodegradable carbamate ester (Vig et al. 2013).

Synthesis of Cyclic RGD Peptide-Drug Conjugates

The cyclic pentapeptide c(RGDfK), first designed and synthesized by Kessler and co-workers (Haubner et al. 1997), was selected as a prototypical delivery vehicle because the lysine side-chain provides a convenient handle for attachment and since diverse relatives are amenable to parallel synthesis (Dai et al. 2000). Apparently, the 5th amino acid side chain residue of c(RGDfK) is not part of the pharmacophore in this peptide (Arap et al. 1998; Goldshaid et al. 2010; Haubner et al. 1997), and therefore it can be substituted with other amino acids like serine, threonine, and aspartic acid, having functional side chains

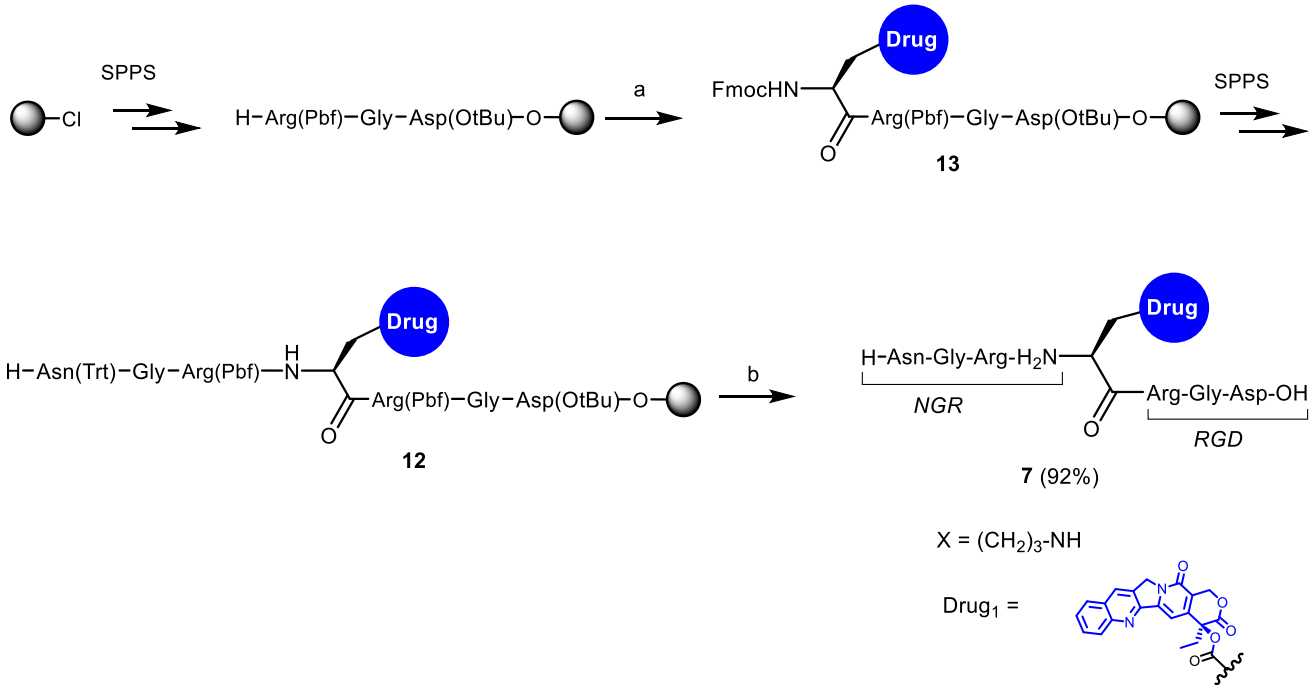

Scheme 4 SPPS of the liner peptide-drug conjugate **7**. *a* 4, PyBop, DIPA/DMF, 3 h, rt; *b* TFA/H_2O/Phenol/TIPS (90:5:3:2), 3 h, rt

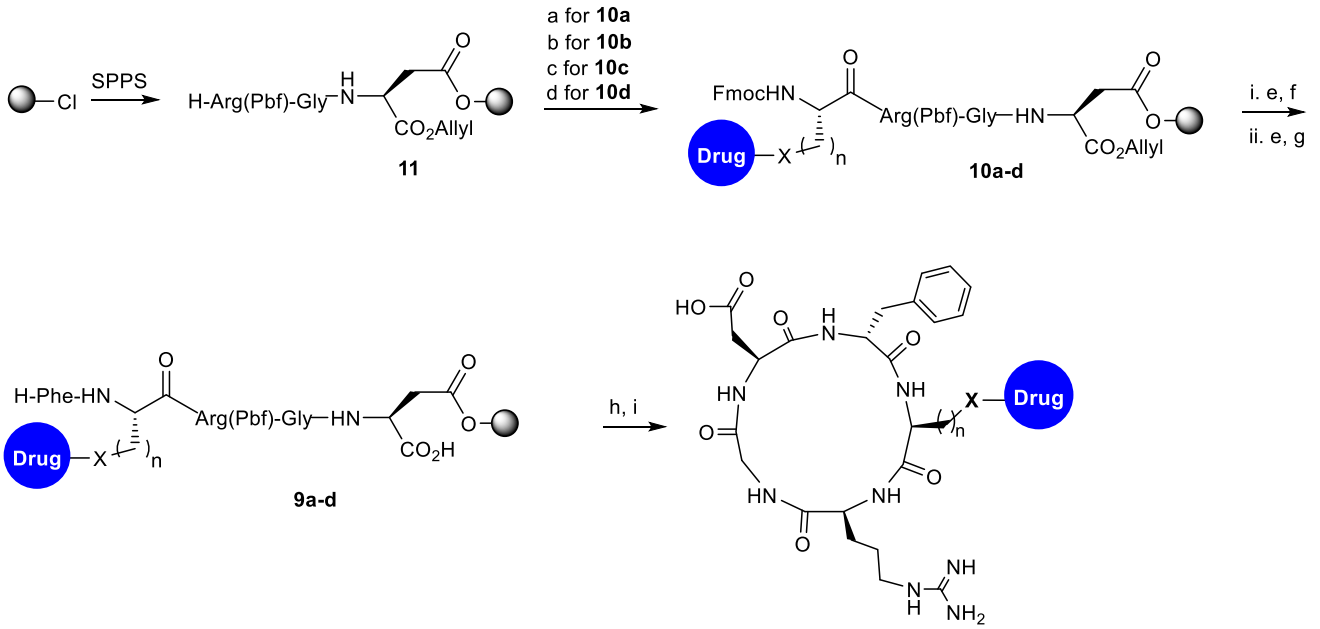

Scheme 5 SPPS of cyclic conjugates **8a–d**. *a–d* HATU, DIPA/DMF, 3 h, rt, 1a for a, 5 for b, 3b for c, 3d for d; *e* 20 % piperidine/DMF; *f* Fmoc-D-Phe, HATU, DIPA/DMF; *g* $Pd(PPh_3)_4$ (0.3 eq.), DMBA (6 eq.); *h* PyBop (5 eq.), HOBt (5 eq.), DIPA (10 eq.)/NMP, overnight, rt; *i* TFA/H_2O/Phenol/TIPS (90 %/5 %/3 %/2 %), 3 h, rt

suitable for drug linkage. We now describe a practical and efficient solid-phase synthesis of 'Kessler type' c(RGDfK), c(RGDfS) and c(RGDfE) peptide-drug conjugates, based on standard Fmoc chemistry protocols, using our BUs. Noteworthy, our proposed BU approach can be utilized for facile incorporation of drugs into peptide conjugates by throughput parallel synthesis.

The synthesis of cyclic conjugates **8a–d**, which covers all three drug-BU linkage functionalities—namely ester, carbamate and amide—were carried out by using four representative AABUs: BU **1** for the ester conjugate, BU **5** for the carbamate conjugate and BUs **3b** and **3d** for the amide conjugates (Scheme 5). Notably, analogs of our cyclic RGD–camptothecin conjugate **8b** were previously described (Dal Pozzo et al. 2010). In that work Dal Pozzo et al. reported on a conjugation of Namitecan and its aldehyde derivatives through an amide and hydrazine linkage moiety to the cyclic RGDfK peptide carrier in solution. We report, on the other hand, on complete SPPS of the peptide-drug conjugate in which camptothecins' linkage to the peptide carrier is through carbamate functionality, thus yielding structurally different conjugate.

The extension of our BUs repertoire, evaluation of peptide/drug/sequence/release profiling and bioactivity of peptide-drug conjugates is currently under investigation.

Cell Cytotoxicity

In order to compare the specific cytotoxic effects of the linear conjugate **7** with its cyclic counterpart **8b**, cytotoxicity assays were performed using three different cell lines: a human non-small cell lung carcinoma cell line H-1299 and a human prostate cancer cell line PC-3, both of which overexpress $\alpha_v\beta_3$ integrins (68 and 69 % respectively, Fig. 2), and a HEK-293 (Human Embryonic Kidney 293) cell line, which served as a negative control with 2 % of $\alpha_v\beta_3$ expression (Fig. 2). The level of $\alpha_v\beta_3$ integrin expression was determined by direct immunofluorescence assay (Fig. 2) as described in materials and methods.

Cells were seeded in micro wells and allowed to adhere during a 24 h incubation period, after which the cultures were washed, fresh medium containing different concentrations of the tested substances was added and subsequently the cultures were incubated for additional 6 h. After removal of the substances containing medium (to avoid non-receptor dependent activity), fresh medium was added and the cells were reincubated for additional 24 h. At the end of the second 24 h incubation period, the mitochondrial activity of the cells was measured by XTT assay. The effect of drug treatment on the mitochondrial activity was expressed as % of growth inhibition (GI)

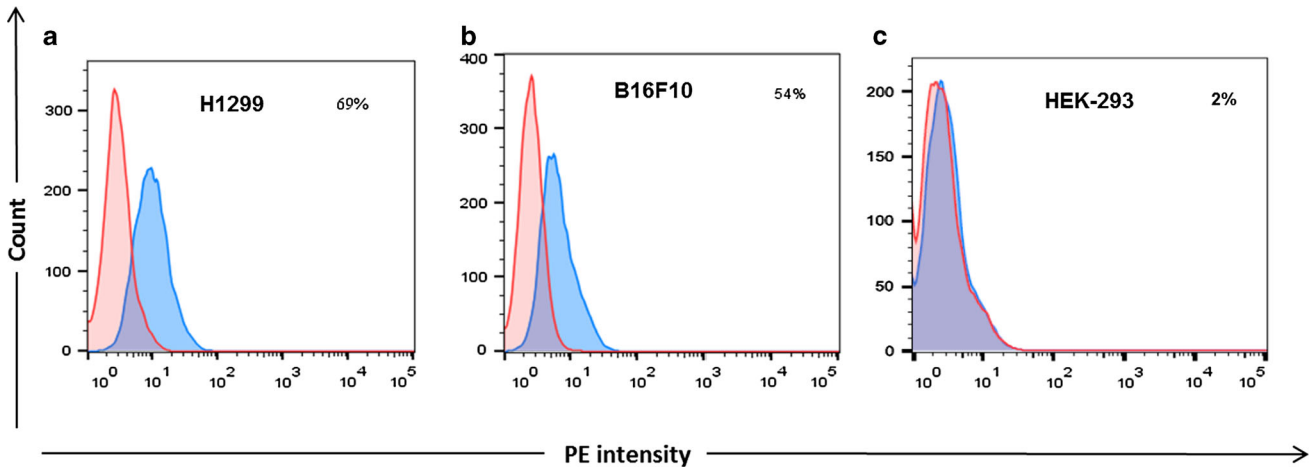

Fig. 2 Flow cytometry analysis of $\alpha_v\beta_3$ integrin expression in **a** H1299, **b** PC-3 and **c** HEK cell lines. In *each graph* the *x axis* represents the intensity of fluorescence and the *y axis* represents the number of counted cells

compared to cells which were exposed only to DMSO (0.05 %) containing medium.

In the in vitro cytotoxicity assay, the free CPT exerted non-specific dose dependent manner of action towards all the tested cell lines, namely H1299, PC-3 and HEK (Fig. 3). Conjugation of this Topo I inhibitor (CPT) to the linear RGD-NGR peptide **7** significantly reduced its toxicity in tested cancer cell lines, but still preserving moderate potency probably due to low affinity of the linear RGD and NGR sequences on $\alpha_v\beta_3$ integrin receptor (Gurrath et al. 1992; Shabbir et al. 2010). On the other hand, the cyclic RGD-CPT conjugate **8b** presented significant toxicity reduction towards $\alpha_v\beta_3$ negative HEK cells, but not towards $\alpha_v\beta_3$ integrin overexpressing H-1299 and PC-3 tumor cells. Moreover, the percentage of growth inhibition (GI) of 8b in PC-3 cells was even higher than the percentage of growth inhibition of a free drug. This tendency was observed as well in H1299 cells, but only at concentrations higher than 50 μM.

Affinity Assay of Conjugate 8b to $\alpha_v\beta_3$ Integrin

In order to assess the correlation between the selective cytotoxicity of conjugate **8b** towards cells with overexpression of the $\alpha_v\beta_3$ integrin and with the affinity of this conjugate (**8b**) to the relevant receptor ($\alpha_v\beta_3$ integrin), an immunofluorescence assay was performed: Cells with overexpressed level of $\alpha_v\beta_3$ were first incubated with solutions containing different concentrations of conjugate

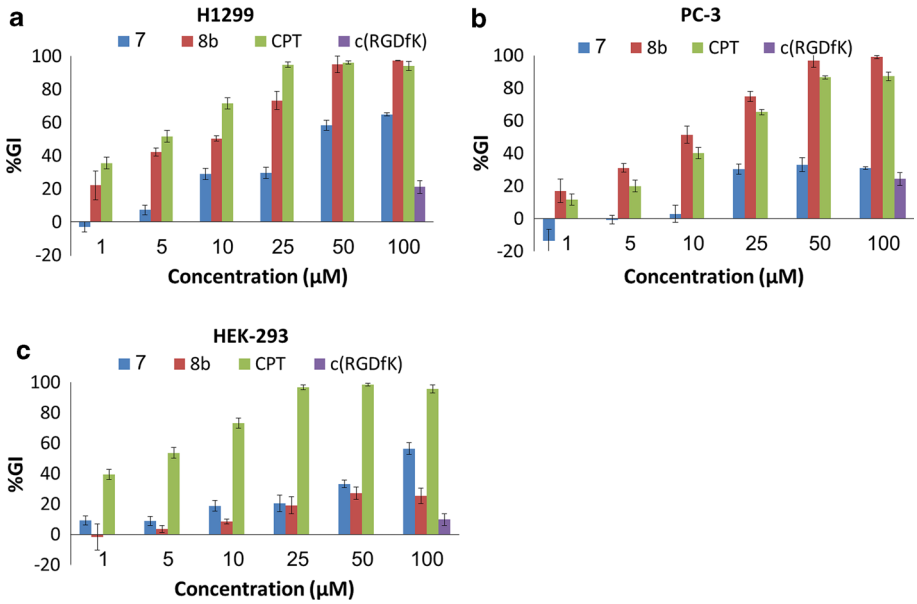

Fig. 3 XTT growth inhibition assay—the effect on cell growth of peptide-CPT-conjugates *vs* a free CPT was studied in three cell lines: **a** H1299 and **b** PC-3 cell lines, which over-express integrin $\alpha_v\beta_3$ and **c** HEK cell line, which is $\alpha_v\beta_3$-negative. The result shown for each concentration point represents the mean ± SD calculated from a quadruplicate

8b. Following this incubation, all the cell samples were centrifuged, washed and then incubated again with uniform amount of R-phycoerythrin-conjugated anti-human CD51/CD61 antibody. At the end of the second incubation period all the cell samples were centrifuged and washed again and then tested for the bound level of CD51/CD61 antibody by FACS cell analyzer (Fig. 2). As seen from Fig. 2, increase in the amount of the conjugate **8b** (first step incubation) results in decrease levels of the bound CD51/CD61 antibody (second step incubation). Being c(RGDfK) an high affinity ligand to the integrin $\alpha_v\beta_3$ receptor was supported by this experiment, which shows that cells with overexpression of $\alpha_v\beta_3$ bound less $\alpha_v\beta_3$ specific antibody if previously incubated with the c(RGDfK)-CPT conjugate (**8b**). Moreover, this observation confirms as well, that also after the conjugation of the drug (CPT) to the peptide core, the affinity of the resulted conjugate (**8b**) to the targeted receptor is preserved. These results support our perception that the selective cytotoxicity of **8b** is mediated by $\alpha_v\beta_3$ integrin receptor (Fig. 4).

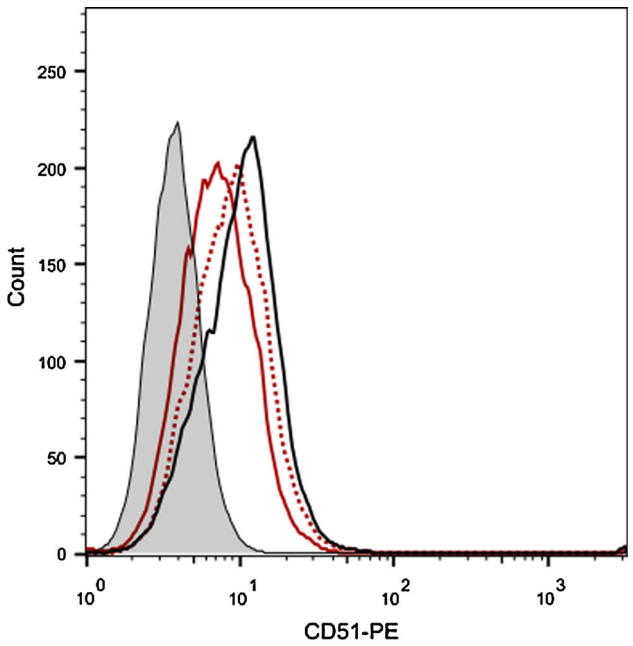

Fig. 4 Flow cytometry analysis of four samples of PC-3 cells: *gray*—unstained cells (control sample); *solid red line*—cells which were incubated with 10 nM of conjugate **8b** then washed and incubated again with R-phycoerythrin-conjugated anti-human CD51/CD61 antibody; *dashed red line*—cells which were incubated with 1 nM of conjugate **8b** then washed and incubated again with R-phycoerythrin-conjugated anti-human CD51/CD61 antibody; *black solid line*—cells which were incubated with R-phycoerythrin-conjugated anti-human CD51/CD61 antibody without be previously incubated with **8b**

Conclusions

In this paper we describe a facile preparation of Fmoc protected amino acid—drug building units for using as structural elements in the divergent synthesis of PDCs. Their simple, practical and efficient implementation in the solid-phase synthesis of novel linear RGD-NGR as well as a 'Kessler like' $a_v\beta_3$ integrin antagonistic conjugates using straight forward Fmoc chemistry was also exemplified. Moreover, our method utilizes the diversity of drug linkages by a facile incorporation into peptide conjugates, applying convergent SPPS. The synthetic routes reported in this work should be amenable to fast parallel synthesis of a wide range of analogous peptide-drug conjugates for fast assessment of drug release profile that depends on the nature of the linker (AA side chain), position in the peptide sequence, linking moiety and the drug itself.

In the in vitro cytotoxicity study, the free CPT was non-specifically cytotoxic to all cell lines, including negative control HEK cells that lack $\alpha_v\beta_3$ integrins. Cyclic RGD-CPT conjugate, on the other hand, exerted selective potency on $\alpha_v\beta_3$ overexpressed cancer cell lines as compared to the negative control HEK cells. In particular, cyclic RGD-CPT was more toxic than free CPT on prostate cancer cells PC-3 in all concentrations. The well know phenomena of being c(RGDfK) a high affinity ligand to the integrin $\alpha_v\beta_3$ was supported in this work by the FACS experiment. Furthermore, these results confirm that after conjugating a drug (CPT) to the peptidic core, the affinity of the resulted conjugate to the targeted receptor is preserved.

A future perspective of incorporation of the discussed AABUs in the backbone of targeted peptide-drug bioconjugates could be an attachment of several types of anticancer drugs - through different linkages—within a single conjugate. This may result in a synergistic action of the drugs in the target and thereby could further enhance the drug delivery for preclinical targeted cancer therapy assessment.

Materials and Methods

General Methods and Cell Lines

The NMR spectral data was recorded in deuterated solvents at 300 MHz—Bruker NMR spectrometer or 400 MHz—Bruker Avance-III 400 MHz NMR spectrometer equipped with a BBFO probe, and reported in δ ppm relative to TMS as an internal standard. Mass spectra was measured using *Autoflex III smartbeam* (*MALDI, Bruker*) in linear or reflectron mode, positive or negative or *Q-TOF micro* (*Waters*) ESI (+ *or* −). HPLC/LC–MS analyses were

collected using C18, 2.1 × 50 mm, 1.8 μm column kept at 50 °C, with detection at 254 nm. The eluent solvents were A (0.1 % TFA in H_2O) and B (0.1 % TFA in ACN). The flow rate was of 0.4 mL/min. The MS fragmentor was tuned on 30 or 70 V on positive or negative mode. For the elution gradient profile see supporting information. All HPLC purifications were done via reverse phase on semi-preparative system with dual UV detection at 254 nm and 230 nm. Phenomenex Gemini® 10 μm C18 110 Å, LC 250 × 21.2 mm prep column was utilized. The eluent solvents were A (0.1 % TFA in H_2O) and B (0.1 % TFA in ACN). The flow rate was set up on 25 mL/min. For the elution gradient profile see supporting information. Thin layer chromatography (TLC) was performed using 20 × 20 cm silica-gel plates (Merck silica gel, 60 F_{254}), and visualized under UV fluorescence (λ_{max} = 254 nm and/or 366 nm). CAMP and CLB were purchased from Tzamal D-Chem Laboratories Ltd. Petah-Tikva, Israel. All the cell lines were cultured in RPMI medium supplemented with L-glutamine, 10 % fetal bovine serum and with penicillin streptomycin (100 IU/mL of each) (cell culture growth medium and all of its additives were purchased from Biological Industries, Bet-Ha'emek, Israel). All cell cultures were grown at a 37 °C incubator in an environment containing 6 % CO_2.

Chemistry

*General Procedure for the Synthesis of **1a–c***

To a suspension of Fmoc–AA–OH (0.5 mmol) in DCM (25 mL) was added DIPA (1.1 eq.) (making the solution clear), followed by addition of 2-Cl-Trt chloride (1.05 mmol). After stirring at rt. for 2 h, the solvent was evaporated, providing a cotton-like product. It was dissolved in DCM and then CLB (1 eq.), HOBt (1.5 eq.), DMAP (1 eq.) and DCC (1.5 eq.) were added and white precipitate was observed after about 20 min. The mixture was allowed to stir overnight. The white precipitate was removed by filtration resulting in a clear pale orange solution. The solvent was removed, and the crude product was dissolved in DCM (30 mL) with a small amount of MeOH. The organic solution was washed several times with H_2O, brine and $NaHCO_3$ (5 %). The collected organic phase was dried over Na_2SO_4, and evaporated, yielding beige oil. The crude was suspended in DCM, TFA was added (to 3 % final concentration) and the beige suspension immediately turns into an orange solution. The mixture was allowed to stir for 1 h. The solvent was removed and the crude was purified by semi-preparative HPLC. Clean fractions were lyophilized resulting oily products in 82, 75, and 73 % yields for Ser, Tyr, and Thr building units respectively.

*[Fmoc–Ser(CLB)–OH] (**1a**)* Compound **1a** was obtained as brownish oil with 82 % yield Rf: 0.72 (25 %MeOH/EtOAc); LC–MS *m/z*: 615 ($M+H^+$), RT = 10.80 min; ^1H NMR (300 MHz, DMSO-d_6): δ 1.88 (t, J = 8.7 Hz, 2H), 2.32 (t, J = 8.7 Hz, 2H), 2.52 (t, J = 8.7 Hz, 2H), 3.58 (t, J = 6.8 Hz, 4H), 3.68 (t, J = 6.8 Hz, 4H), 4.25 (t, J = 8.1 Hz, 1H), 4.35 (d, J = 8.1 Hz, 2H), 4.45 (m, 1H), 4.65 (m, 1H), 5.65 (d, J = 8.0 Hz, 1H), 6.8 (d, J = 8.0 Hz, 2H), 7.2 (d, J = 8.0 Hz, 2H), 7.3 (t, J = 8.0 Hz, 2H), 7.39 (t, J = 8.0 Hz, 2H), 7.58 (d, J = 8.0 Hz, 2H), 7.75 (d, J = 8.0 Hz, 2H); HRMS: ESI–MS *m/z* calcd: 613.1832, found: 613.1834 (MH^+).

*[Fmoc–Thr(CLB)–OH] (**1b**)* Compound **1b** was obtained as brownish oil with 73 % yield Rf: 0.79 (25 %MeOH/EtOAc); LC–MS *m/z*: 627 ($M+H^+$), RT = 11.05 min; ^1H NMR (400 MHz, DMSO-d_6): δ 1.21 (br. s, 3H); 1.75 (br. quint, 2H), 2.24 (br. q, 2H), 2.43 (br. q, 2H), 3.68 (s, 8H), 4.24 (m, 4H), 5.25 (m, 1H), 6.64 (d, J = 8.6 Hz, 2H), 7.00 (d, J = 8.6 Hz, 2H), 7.32 (t, J = 6.9 Hz, 2H), 7.41 (t, J = 6.9 Hz, 2H), 7.77 (d, J = 6.9 Hz, 2H), 7.90 (d, J = 6.9 Hz, 2H); HRMS: ESI–MS *m/z* calcd: 649.189, found: 649.185 ($M+Na^+$), calcd: 665.159, 665.166 ($M+K^+$).

*[Fmoc–Tyr(CLB)–OH] (**1c**)* Compound **1c** was obtained as brownish oil with 75 % yield Rf: 0.80 (25 % MeOH/EtOAc); LC–MS *m/z*: 689 ($M+H^+$), RT = 11.10 min; ^1H NMR (300 MHz, DMSO-d_6): δ 1.88 (quint, J = 7.6 Hz 2H), 2.55 (m, 4H), 2.87 (dd, J = 14.0, 7.6 Hz 1H), 3.08 (dd, J = 14.0, 7.6 Hz 1H), 3.7 (s, 8H), 4.2 (m, 4H), 6.65 (d, J = 8 Hz, 2H), 7.0 (d, J = 8 Hz, 2H), 7.06 (d, J = 8 Hz, 2H), 7.28 (m, 2H), 7.31 (m, 2H), 7.4 (m, 2H), 7.65 (t, J = 8 Hz, 2H), 7.74 (d, J = 8 Hz, 1H), 7.87 (d, J = 8 Hz, 2H); **HRMS**: ESI–MS *m/z* calcd: 711.205, found: 711.193 ($M+Na^+$).

*General Procedure for the Synthesis of **4a–l**: PyBop Method*

Fmoc–AA–OtBu/OAllyl (0.5 mol) was stirred in 10 mL of DMF and then DIPA (3 eq.) was added. Into the resulted clear solution of the AA carboxylate the coupling reagent PyBop (1 eq.) was added. Into this stirred active ester solution the drug with a free amine group was added immediately and the mixture allowed to stir at rt. Aliquots of the reaction solution were monitored by LC–MS and after a completion of the reaction—typically after 3 h—the reaction solution was directly subjected to purification by semi prep. HPLC. Clean fractions were lyophilized resulting powdery product.

*General Procedure for the Synthesis of **4a–l**: IBCF (Asymmetric Anhydride) Method*

Fmoc–AA–OtBu/OAllyl (0.5 mol) was dissolved in 5 mL of THF containing 1.1 eq. of TEA. The carboxylate solution was cooled to (−15) °C to (−20) °C following IBCF addition. After 15 min to the cool white suspended solution the drug with a free amine group—dissolved in a minimal amount of DMSO—was added and the mixture stirred for 30 min in the cool bath following 3–7 h of stirring at rt. If needed, portions of DMSO were added in order to result clear solution. After the LC–MS monitoring indicated that the reaction was completed, the mixture was subjected to purification by semi prep. HPLC. Clean fractions were lyophilized resulting crystalline powders.

*[Fmoc–Asp(Deacetyl Colchicine)–OtBu] (**4a**)* Compound **4a** was obtained as yellow solid with 63 % yield by PyBop coupling method or 78 % yield by IBCF asymmetric anhydride method. ^{1}H NMR: (400 MHz, DMSO-d_6): δ 1.32 (s, 9H), 1.79–1.87 (m, 1H), 1.96–2.02 (m, 1H), 2.18–2.27 (m, 1H), 2.54–2.61 (m, 3H), 3.53 (s, 3H), 3.78 (s, 3H), 3.82 (s, 3H), 3.86 (s, 3H), 4.15–4.29 (m, 4H), 4.30–4.40 (m, 1H), 6.76 (s, 1H), 7.01–7.13 (m, 2H), 7.16 (s, 1H), 7.40 (t, J = 8.0 Hz, 2H) 7.59 (d, J = 7.0 Hz, 1H), 7.66 (dd, 7.5, 3 Hz, 2H) 7.88 (d, J = 7.0 Hz, 2H), 8.58 (d, J = 7.0 Hz, 1H); ^{13}C and DEPTQ (^{13}C) NMR (101 MHz, DMSO-d_6): δ 27.39 (3 CH_3), 29.10 (CH_2), 30.31 (C), 35.79 (CH_2), 36.83 (CH_2), 46.46 (CH), 51.12 (CH), 51.26 (CH), 55.72 (CH_3), 55.93 (CH_3), 60.58 (CH_3), 60.72 (CH_3), 65.53 (CH_2), 107.72 (CH), 111.96 (CH), 120.00 (2 CH), 125.08(CH), 125.10 (CH), 125.30 (C), 126.92 (2 CH), 127.50 (CH), 127.51 (CH), 130.39 (CH), 134.06 (C), 134.27 (CH), 134.98 (C), 140.59 (C), 140.65 (C), 143.64 (2 C), 143.68 (C), 150.32 (C), 150.35 (C), 152.86 (C), 156.60 (CO–NH-OR), 163.42 (C), 168.07 (CO-OR), 170.55 (CO-NHR), 177.89 (CO); LC–MS *m/z*: 751 ($M+H^+$), RT = 10.70 min.

*[Fmoc–Glu(Deacetyl colchicine)–OtBu] (**4b**)* Compound **4b** was obtained as yellow solid with 64 % yield by PyBop coupling method or 80 % yield by IBCF asymmetric anhydride method. ^{1}H NMR: (400 MHz, DMSO-d_6): δ 1.36 (s, 9H), 1.65–1.75 (m, 1H), 1.78–1.92 (m, 2H), 1.96–2.06 (m, 1H), 2.17–2.30 (m, 3H), 2.59 (dd, J = 13.0, 7.0 Hz, 2H), 3.53 (s, 3H), 3.79 (s, 3H), 3.83 (s, 3H), 3.87 (s, 3H), 4.20–4.37 (m, 4H), 6.67 (s, 1H) 7.01–7.14 (m, 3H), 7.33 (t, J = 7.5 Hz, 2H) 7.43 (t, J = 7.5 Hz, 2H), 7.69 (s, 1H) 7.72 (d, J = 7.5 Hz, 2H), 7.90 (d, J = 7.5 Hz, 2H), 8.58 (d, J = 5.5 Hz, 1H); ^{13}C NMR (101 MHz, DMSO-d_6): δ 26.30 (CH_2), 27.51 (3 CH_3), 29.11 (CH_2), 31.31 (C), 35.65 (CH_2), 46.55 (CH), 51.13 (CH), 51.93 (CH), 55.74 (CH_3), 55.93 (CH_3), 60.59 (CH_3), 60.75 (CH_3), 65.53 (CH_2), 107.62 (CH), 112.01 (CH), 120.03 (2 CH), 125.17 (2 CH), 125.33 (C), 126.98 (2 CH), 127.56 (2 CH), 130.26 (CH), 134.13 (C), 134.31 (CH), 135.07 (C), 140.63 (2 C), 143.70 (2 C), 143.71 (C), 150.34 (C), 150.66 (C), 152.84 (C), 156.00 (CO–NH-OR), 163.43 (C), 170.50 (CO-OR), 171.24 (CO-NHR), 177.89 (CO); LC–MS *m/z*: 765 ($M+H^+$), RT = 10.33 min.

*[Fmoc–Asp(Amonafide)–OtBu] (**4c**)* Compound **4c** was obtained as orange solid with 70 % yield by PyBop coupling method or 75 % yield by IBCF asymmetric anhydride method. ^{1}H NMR: (400 MHz, DMSO-d_6): δ 1.36 (s, 9H), 2.77 (dd, J = 16.0, 6.0 Hz, 1H), 2.91 (s, 3H), 2.92 (s, 3H), 2.96 (dd, J = 16.0, 6.0 Hz, 1H), 3.44–3.49 (br. q, 2H), 4.23 (t, 7.0 Hz, 1H), 4.30–4.36 (m, 2H), 4.39 (t, J = 5.0 Hz, 2H), 4.67 (q, J = 7.0 Hz, 1H), 7.31 (t, J = 7.0 Hz, 2H), 7.40 (t, J = 7.5 Hz, 2H), 7.71 (dd, J = 8.0, 1.0 Hz, 2H), 7.82–7.86 (m, 2H), 7.89 (d, J = 7.0 Hz, 2H), 8.70 (d, J = 2.0 Hz, 1H), 8.77 (d, J = 2.0 Hz, 1H), 9.26 (s, 1H), 10.71 (s, 1H); LC–MS *m/z*: 677 ($M+H^+$), RT = 9.49 min.

*[Fmoc–Glu(Amonafide)–OtBu] (**4d**)* Compound **4d** was obtained as orange solid with 78 % yield by PyBop coupling method or 81 % yield by IBCF asymmetric anhydride method. ^{1}H NMR: (400 MHz, DMSO-d_6): δ 1.42 (s, 9H), 1.89–1.95 (m, 1H), 2.11–2.16 (m, 1H), 2.56 (t, J = 5.5 Hz, 2H), 2.91 (s, 3H), 2.92 (s, 3H), 3.43–3.48 (m, 2H), 4.01–4.06 (m, 1H), 4.19–4.36 (m, 3H), 4.38 (t, J = 5.5 Hz, 2H), 7.33 (t, J = 7.5 Hz, 2H) 7.42 (t, J = 7.5 Hz, 2H), 7.73 (d, J = 7.5 Hz, 2H), 7.77–7.85 (m, 2H), 7.89 (d, J = 7.5 Hz, 2H), 8.37–8.41 (m, 2H), 8.68 (d, J = 2 Hz, 1H), 8.77 (d, J = 2 Hz, 1H), 9.30 (s, 1H), 10.61 (s, 1H); ^{13}C and DEPTQ (^{13}C) NMR (101 MHz, DMSO-d_6): δ 26.04 (CH_2), 27.56 (3 CH_3), 32.50 (CH_2), 35.07 (CH_2), 42.67 (2 CH_3), 46.55 (CH), 53.85 (CH), 54.84 (CH_2), 64.53 (CH_2), 80.59 (C), 120.03 (2 CH), 120.75 (CH), 121.85 (C), 122.64 (C), 123.80 (CH), 124.00 (C), 125.13(2 CH), 126.96 (2 CH), 127.51 (CH), 127.55 (2 CH), 128.94 (CH), 132.01 (C), 133.81 (CH), 137.90 (C), 140.62 (C), 140.63 (C), 143.67 (C), 143.71 (C), 156.07 (CO–NH–OR), 163.70 (CO–NR–CO), 163.95 (CO–NR–CO), 171.04 (CO–OH), 171.29 (CO–NHR); LC–MS *m/z*: 691 ($M+H^+$), RT = 9.30 min.

*[Fmoc–Asp(Cytarabine)–OtBu] (**4e**)* Compound **4e** was obtained as white solid with 72 % yield by IBCF asymmetric anhydride method. ^{1}H NMR: (400 MHz, DMSO-d_6): δ 1.39 (s, 9H), 2.74 (dd, J = 15, 6 Hz), 2.91 (dd, J = 15, 6 Hz), 3.62 (d, J = 5.4 Hz, 2H), 3.81–3.86 (m, 1H), 3.93 (t, J = 3.1 Hz, 1H), 4.07 (dd, J = 4, 2.5 Hz, 1H), 4.23 (d, J = 7.0 Hz, 1H), 4.29 (s, 1H), 4.31 (br quart, 1H), 4.39 (dd, J = 15.0, 7.0 Hz, 1H), 5.00–5.90 (br s, 3 [OH]),

6.05 (d, J = 4.0 Hz, 1H), 7.19 (d, J = 7.5 Hz, 1H), 7.32 (dt, J = 7.5, 1.2 Hz, 2H), 7.42 (t, J = 7.5 Hz, 2H), 7.71 (d, J = 7.5 Hz, 2H), 7.80 (d, J = 7.5 Hz, 1H), 7.89 (d, J = 7.5 Hz, 2H), 8.08 (d, J = 7.5 Hz, 1H), 10.95 (s, 1H); ^{13}C and DEPTQ (^{13}C) NMR (400 MHz, DMSO-d_6): δ 27.43 (3 CH_3), 35.75 (CH_2), 38.37 (CH_2), 46.48 (CH), 50.67 (CH), 60.91 (CH_2), 65.59 (CH_2), 74.47 (CH), 76.02 (CH), 80.81 (C), 85.69 (CH), 86.93 (CH), 94.22 (CH), 120.02 (2 CH), 125.12 (2 CH), 126.96 (2 CH), 127.54 (2 CH), 140.61 (2 C), 143.66 (2 C), 146.76 (CH), 154.31 (CO-(NR_2)$_2$), 155.72 (CO-NHR-OR), 161.94 (C), 170.15 (CO-OR), 170.49 (CO-NHR); LC–MS *m/z*: 637 ($M+H^+$), RT = 9.58 min.

[Fmoc–Glu(Cytarabine)–OtBu] (4f) Compound **4f** was obtained as white solid with 76 % yield by IBCF asymmetric anhydride method. ^{1}H NMR: (400 MHz, DMSO-d_6): δ 1.40 (s, 9H), 1.73–1.90 (m, 1H), 1.93–2.06 (m, 1H), 2.51–2.55 (m, 2H), 3.62 (d, J = 5.4 Hz, 2H), 3.70–4.10 (br s, 3 [OH]), 3.81–3.86 (m, 1H), 3.93 (t, J = 3.1 Hz, 1H), 4.07 (dd, J = 4.0, 2.5 Hz, 1H), 4.20–4.36 (m, 3H), 6.06 (d, 4.0 Hz, 1H), 7.20 (d, J = 7.5 Hz, 1H), 7.34 (dt, J = 7.5, 1.2 Hz, 2H), 7.42 (t, J = 7.5 Hz, 2H), 7.70 (d, J = 7.5 Hz, 1H), 7.73 (d, J = 7.5 Hz, 2H), 7.90 (d, J = 7.5 Hz, 2H), 8.07 (d, J = 7.5 Hz, 1H), 10.98 (s, 1H); ^{13}C and DEPTQ (^{13}C) NMR (400 MHz, DMSO-d_6): δ 25.60 (CH_2), 27.52 (3 CH_3), 32.67 (CH_2), 46.53 (CH), 53.68 (CH), 60.91 (CH_2), 65.52 (CH_2), 74.48 (CH), 76.01 (CH), 80.59 (C), 85.66 (CH), 86.88 (CH), 94.19 (CH), 120.03(2 CH), 125.14 (2 CH), 126.98 (2 CH), 127.55 (2 CH), 140.63 (2 C), 143.68 (C), 143.69 (C), 146.66 (CH), 154.34 (CO–(NR_2)$_2$), 155.98 (CO–NHR–OR), 161.97 (C), 171.18 (CO–OR), 172.78 (CO–NHR); LC–MS *m/z*: 651 ($M+H^+$), RT = 9.58 min.

[Fmoc–Asp(Deacetyl Colchicine)–OAllyl] (4g) Compound **4g** was obtained as yellow solid with 72 % yield by PyBop coupling method or 70 % yield by IBCF asymmetric anhydride method.^{1}H NMR: (400 MHz, DMSO-d_6): δ 1.78–1.87 (m, 1H), 1.95–2.05 (m, 1H), 2.17–2.26 (m, 1H), 2.54–2.72 (m, 3H), 3.53 (s, 3H), 3.79 (s, 3H), 3.83 (s, 3H), 3.87 (s, 3H), 4.18–4.29 (m, 3H), 4.34–4.44 (m, 2H), 4.50–4.60 (m, 2H), 5.10 (dq, J = 11.0, 2.0 Hz, 1H), 5.23 (dq, J = 17.0, 2.0 Hz, 1H), 5.75–5.85 (m, 1H), 6.76 (s, 1H), 7.02 (d, 7.0 Hz, 1H), 7.12 (d, 7.0 Hz, 1H), 7.16 (s, 1H), 7.25–7.30 (m, 2H), 7.40 (t, J = 7.5 Hz, 2H) 7.66 (dd, J = 7.5, 2.5 Hz, 2H), 7.76 (d, 7.0 Hz, 1H), 7.88 (d, J = 7.0 Hz, 2H), 8.58 (d, J = 7.0 Hz, 1H); ^{13}C and DEPTQ (^{13}C) NMR (400 MHz, DMSO-d_6): δ 29.10 (CH_2), 35.75 (CH_2), 36.72 (CH_2), 46.44 (CH), 50.40 (CH), 51.25 (CH), 55.73 (CH_3), 55.94 (CH_3), 60.59 (CH_3), 60.76 (CH_3), 64.85 (CH_2), 65.61 (CH_2), 107.62 (CH), 111.98 (CH), 117.38 (CH), 120.02(2 CH), 125.08 (2 CH), 125.30 (CH_2), 126.94 (2 CH), 127.52 (2 CH), 130.36 (CH), 132.16 (CH), 134.07 (C), 134.33 (CH), 134.99 (C), 140.60 (2 C), 140.65 (C), 143.62 (C), 143.66 (C), 150.32 (C), 150.35 (C), 152.86 (C), 155.65 (CO–NH-OR), 163.43 (C), 167.94 (CO-OR), 171.05 (CO-NHR), 177.92 (CO); LC–MS *m/z*: 735 ($M+H^+$), RT = 10.26 min.

[Fmoc–Glu(Deacetyl Colchicine)–OAllyl] (4h) Compound **4h** was obtained as yellow solid with 70 % yield by PyBop coupling method or 74 % yield by IBCF asymmetric anhydride method. ^{1}H NMR: (400 MHz, DMSO-d_6): δ 1.71–1.85 (m, 2H), 1.95–2.04 (m, 2H), 2.17–2.24 (m, 1H), 2.28 (t, 8 Hz 2H) 2.54–2.61 (m, 1H), 3.53 (s, 3H), 3.79 (s, 3H), 3.83 (s, 3H), 3.87 (s, 3H), 4.00–4.06 (m, 1H), 4.20–4.37 (m, 4H), 4.55 (td, 5, 1.5 Hz, 2H), 5.10 (dq, J = 11.0, 2.0 Hz, 1H), 5.23 (dq, J = 17.0, 2.0 Hz, 1H), 5.82–5.91 (m, 1H), 6.77 (s, 1H), 7.02 (d, 7.0 Hz, 1H), 7.11 (d, 7.0 Hz, 1H), 7.13 (s, 1H), 7.33 (t, J = 7.5 Hz, 2H), 7.42 (t, J = 7.5 Hz, 2H), 7.71 (d, J = 7.5 Hz, 2H), 7.84 (d, J = 7.0 Hz, 2H), 7.90 (d, J = 7.5 Hz, 2H), 8.59 (d, J = 7.0 Hz, 1H); DEPTQ (^{13}C) NMR (400 MHz, DMSO-d_6): δ 26.08 (CH_2), 28.92 (CH_2), 31.06 (CH_2), 35.60 (CH_2), 46.50 (CH), 51.10 (CH), 53.30 (CH), 55.70 (CH_3), 55.92 (CH_3), 60.59 (CH_3), 60.76 (CH_3), 64.72 (CH_2), 65.60 (CH_2), 107.62 (CH), 112.01 (CH), 117.60 (CH), 120.02(2 CH), 125.15 (2 CH), 125.30 (CH_2), 126.99 (2 CH), 127.56 (2 CH), 130.25 (CH), 132.24 (CH), 134.12 (C), 134.33 (CH), 135.06 (C), 140.61 (2 C), 143.67 (2 C), 150.32 (C), 150.65 (2 C), 152.83 (C), 156.03 (CO–NH-OR), 163.43 (C), 170.39 (CO-OR), 171.71 (CO–NHR), 177.88 (CO); LC–MS *m/z*: 749 ($M+H^+$), RT = 10.43 min.

[Fmoc–Asp(Amonafide)–OAllyl] (4i) Compound **4i** was obtained as brownish solid with 82 % yield by PyBop coupling method or 84 % yield by IBCF asymmetric anhydride method. ^{1}HNMR: (400 MHz, DMSO-d_6): δ 2.88 (dd, J = 16.0, 6.0 Hz, 1H), 2.91 (s, 3H), 2.92 (s, 3H), 3.04 (dd, J = 16.0, 6.0 Hz, 1H), 3.44–3.49 (br. q, 2H), 4.22 (t, 7.0 Hz, 1H), 4.31–4.36 (m, 2H), 4.39 (t, J = 5.0 Hz, 2H), 4.61 (td, J = 5.0, 1.5 Hz, 2H), 4.67 (q, J = 7.0 Hz, 1H), 5.17 (dq, J = 11.0, 2.0 Hz, 1H), 5.31 (dq, J = 11.0, 2.0 Hz, 1H), 5.83–5.93 (m, 1H), 7.30 (t, J = 7.5, 2H) 7.39 (t, J = 7.5 Hz, 2H), 7.70 (dd, J = 7.0, 3.0 Hz, 2H), 7.84 (t, J = 7.0 Hz, 1H), 7.88 (d, J = 7.0 Hz, 2H), 7.99 (d, J = 7.0 Hz, 2H), 8.40 (dt, J = 8.0, 1.0 Hz, 2H), 8.68 (d, J = 2.0 Hz, 1H), 8.70 (d, J = 2.0 Hz, 1H), 9.31 (s, 1H), 10.74 (s, 1H); ^{13}C and DEPTQ (^{13}C) NMR (101 MHz, DMSO-d_6): δ 35.08 (CH_2), 38.03 (CH_2), 42.67 (2 CH_3), 46.67 (CH), 50.39 (CH), 54.84 (CH_2), 64.98 (CH_2), 65.66 (CH_2), 117.42 (CH_2), 120.02 (2 CH), 120.93 (CH), 121.87 (C), 122.66 (C), 123.80 (CH), 124.10 (C), 125.06(2 CH), 126.96 (2 CH), 127.53 (2 CH), 127.56 (CH), 129.04 (CH), 131.98 (C), 132.16 (CH), 133.86 (CH). 137.70 (C), 140.61

(2 C), 143.60 (C), 143.64 (C), 155.81 (CO–NH–OR), 163.68 (CO–NR–CO), 163.94 (CO-NR-CO), 167.57 (CO-OR), 170.95 (CO–NHR); LC–MS *m/z*: 661 ($M+H^+$), RT = 9.26 min.

*[Fmoc–Glu(Amonafide)–OAllyl] (**4j**)* Compound **4j** was obtained as brownish solid with 79 % yield by PyBop coupling method or 83 % yield by IBCF asymmetric anhydride method. ^{1}H NMR: (400 MHz, DMSO-d_6): δ 1.93–2.01 (m, 1H), 2.16–2.24 (m, 1H), 2.59 (t, J = 5.5 Hz, 2H), 2.91 (s, 3H), 2.92 (s, 3H), 3.38–3.44 (br. q, 2H), 4.19–4.36 (m, 4H), 4.39 (t, J = 5.5 Hz, 2H), 4.62 (td, J = 5, 2 Hz, 3H), 5.21 (dq, J = 11.0, 2.0 Hz, 1H), 5.33 (dq, J = 11.0, 2.0 Hz, 1H), 5.87–5.97 (m, 1H), 7.33 (t, J = 7.5 Hz, 2H) 7.42 (t, J = 7.5 Hz, 2H), 7.72 (d, J = 7.5 Hz, 2H), 7.83 (t, J = 7.5 Hz, 1H), 7.89 (d, J = 7.5 Hz, 2H), 7.93 (d, J = 7.5 Hz, 1H), 8.37–8.41 (m, 2H), 8.68 (d, J = 2 Hz, 1H), 8.76 (d, J = 2 Hz, 1H), 9.34 (s, 1H), 10.63 (s, 1H); ^{13}C and DEPTQ (^{13}C) NMR (101 MHz, DMSO-d_6): δ 25.97 (CH_2), 32.44 (CH_2), 35.07 (CH_2), 42.63 (2 CH_3), 46.51 (CH), 53.30 (CH), 54.82 (CH_2), 64.81 (CH_2), 65.62 (CH_2), 117.63 (CH_2), 120.03 (2 CH), 120.75 (CH), 121.84 (C), 122.63 (C), 123.79 (CH), 124.00 (C), 125.11(2 CH), 126.97 (2 CH), 127.50 (CH), 127.55 (2 CH), 128.93 (CH), 132.00 (C), 132.28 (CH), 133.82 (CH). 137.88 (C), 140.62 (C), 140.63 (C), 143.64 (C), 143.67 (C), 156.12 (CO–NH-OR), 163.69 (CO-NR-CO), 163.94 (CO-NR-CO), 170.98 (CO-OR), 171.75 (CO-NHR); LC–MS *m/z*: 676 ($M+H^+$), RT = 9.29 min.

*[Fmoc–Asp(Cytarabine)–OAllyl] (**4k**)* Compound **4k** was obtained as white solid with 81 % yield by IBCF asymmetric anhydride method. ^{1}H NMR: (400 MHz, DMSO-d_6): δ 2.84 (dd, J = 14, 8 Hz, 1H), 3.00 (dd, J = 16, 6 Hz, 1H), 3.63 (d, J = 5.4 Hz, 2H), 3.83–3.87 (m, 1H), 3.94 (t, J = 3.1 Hz, 1H), 4.08 (dd, J = 4, 2.5 Hz, 1H), 4.24 (d, J = 7 Hz, 1H), 4.31 (br q, 1H), 4.33 (br q, 1H), 4.58 (td, J = 5.0, 2.0 Hz, 2H), 4.76 (br s [3 OH]), 5.18 (dq, J = 10.5, 1.5 Hz, 1H), 5.30 (dq, J = 17.5, 1.7 Hz, 1H), 5.82–5.91 (m, 1H), 6.07 (d, 4.0 Hz, 1H), 7.18 (d, J = 7.5 Hz, 1H), 7.32 (dt, J = 7.5, 1.2 Hz, 2H), 7.42 (t, J = 7.5 Hz, 2H), 7.7 (d, J = 7.5 Hz, 2H), 7.89 (d, J = 7.5 Hz, 2H), 7.94 (d, J = 8.1 Hz, 1H), 8.09 (d, J = 7.5 Hz, 1H), 10.98 (s, 1H); DEPTQ (^{13}C) NMR (101 MHz, DMSO-d_6): δ 25.52 (CH_2), 32.61 (CH_2), 46.51 (CH), 53.12 (CH), 60.90 (CH_2), 64.81 (CH_2), 65.61 (CH_2), 74.48 (CH), 76.00 (CH), 85.67 (CH), 86.90 (CH), 94.20 (CH), 117.66 (CH_2), 120.04(2 CH), 125.13 (2 CH), 127.00 (2 CH), 127.56 (2 CH), 132.25 (CH) 140.63 (2 C), 143.66 (2 C), 146.70 (CH), 154.31 (CO-(NR_2)$_2$), 156.06 (CO-NHR-OR), 161.93 (C), 171.67 (CO–OR), 172.76 (CO–NHR); LC–MS *m/z*: 621 ($M+H^+$), RT = 9.23 min.

*[Fmoc–Glu(Cytarabine)–OAllyl] (**4l**)* Compound **4l** was obtained as white solid with 84 % yield by IBCF asymmetric anhydride method. ^{1}H NMR: (400 MHz, DMSO-d_6): δ 1.81–1.91 (m, 1H), 2.03–2.12 (m, 1H), 2.52–2.56 (m, 2H), 3.62 (d, J = 5.5 Hz, 2H), 3.82–3.85 (m, 1H), 3.93 (t, J = 2.5 Hz, 1H), 4.06–4.12 (m, 2H), 4.24 (d, J = 7 Hz, 1H), 4.29–4.35 (m, 2H), 4.50 (br s, [3 OH]), 4.58 (td, J = 5.0, 2.0 Hz, 2H), 5.20 (dq, J = 10.5, 1.5 Hz, 1H), 5.31 (dq, J = 17.5, 1.5 Hz, 1H), 5.85–5.95 (m, 1H), 6.06 (d, 5.0 Hz, 1H), 7.19 (d, J = 7.5 Hz, 1H), 7.34 (tt, J = 7.5, 1.2 Hz, 2H), 7.42 (t, J = 7.5 Hz, 2H), 7.72 (d, J = 7.5 Hz, 2H), 7.85 (d, J = 7.5 Hz, 1H), 7.90 (d, J = 8.1 Hz, 1H), 8.08 (d, J = 7.5 Hz, 1H), 10.88 (s, 1H); ^{13}C and DEPTQ (^{13}C) NMR (101 MHz, DMSO-d_6): δ 37.98 (CH_2), 46.46 (CH), 50.00 (CH), 60.89 (CH_2), 64.97 (CH_2), 65.71 (CH_2), 74.49 (CH), 76.02 (CH), 85.70 (CH), 86.95 (CH), 94.28 (CH), 117.41 (CH_2), 120.03 (2 CH), 125.10 (2 CH), 126.98 (2 CH), 127.55 (2 CH), 132.11 (CH) 140.62 (2 C), 143.72 (2 C), 146.77 (CH), 154.22 (CO–(NR_2)$_2$), 155.68 (CO–NHR–OR), 161.96 (C), 170.26 (CO–OR), 170.71 (CO–NHR); LC–MS *m/z*: 635 ($M+H^+$), RT = 9.30 min.

*General Procedures of the Synthesis of **3a–f***

For compounds **4a–4f**, the purified Fmoc–AA(drug)–OtBu was dissolved in 4–7 mL of TFA/DCM 9/1. The concentrated TFA solution was stirred for 2 h, after which the solvent was removed under a gentle N_2 flow resulting in an oily crude. Fmoc–AA(drug)–OH was obtained in a form of crystal powder after precipitation from diethyl ether.

For compounds **4g–4l**, the purified Fmoc–AA(drug)–OAllyl was dissolved in 10 mL of DCM. Then 0.3 eq. of $Pd(PPh_3)_4$ and 3 eq. of DMBA were added, and the mixture was allowed to stir for 4 h at rt after what the solvent was removed under reduced pressure and the resulted oily crude was redissolved in ACN or DMF and then subjected to purification by semi prep. HPLC. Clean fractions where lyophilized to resulting Fmoc–AA(drug)–OH BUs as crystalline powder.

*[Fmoc–Asp(Deacetyl Colchicine)–OH] (**3a**)* Compound **3a** was obtained as pale yellow solid with 90 % yield from 4a or with 58 % yield from 4 g. ^{1}H NMR: (400 MHz, DMSO-d_6): δ 1.76–1.90 (m, 1H), 1.91–2.04 (m, 1H), 2.14–2.29 (m, 1H), 2.53–2.64 (m, 3H), 3.53 (s, 3H), 3.78 (s, 3H), 3.82 (s, 3H), 3.86 (s, 3H), 4.16–4.21 (m, 4H), 4.31–4.39 (m, 1H), 6.75 (s, 1H), 7.01 (d, J = 11.5 Hz, 1H), 7.10 (d, J = 11.5 Hz, 1H), 7.16 (s, 1H), 7.26 (m, 2H), 7.39 (t, J = 8.0 Hz, 2H) 7.55 (d, J = 7.0 Hz, 1H), 7.66 (dd, 7.5, 3.0 Hz, 2H) 7.88 (d, J = 7.0 Hz, 2H), 8.58 (d, J = 7.0 Hz, 1H); DEPTQ (^{13}C) NMR (101 MHz, DMSO-d_6): δ 29.10 (CH_2), 35.75 (CH_2), 36.66 (CH_2), 46.44 (CH), 50.26 (CH), 55.70 (CH_3), 55.92 (CH_3), 60.58 (CH_3), 60.77 (CH_3), 65.54

(CH_2), 107.60 (CH), 111.94 (CH), 119.99 (2 CH), 125.11(CH), 125.14 (CH), 125.27 (C), 126.93 (2 CH), 127.49 (2 CH), 130.35 (CH), 134.06 (C), 134.27 (CH), 134.97 (C), 140.56 (2 C), 140.63 (C), 143.64 (C), 143.71 (C) 150.29 (C), 150.34 (C), 152.85 (C), 155.61 (CO–NH–OR), 163.40 (C), 168.30 (CO–OH), 172.93 (CO–NHR), 177.91 (CO); LC–MS *m/z*: 695 ($M+H^+$), RT = 9.19 min.

*[Fmoc–Glu(Deacetyl Colchicine)–OH] (**3b**)* Compound **3b** was obtained as pale yellow solid with 91 % yield from 4b or with 51 % yield from 4 h. ^{1}H NMR: (400 MHz, DMSO-d_6): δ 1.66–1.88 (m, 2H), 1.88–2.09 (m, 2H), 2.16–2.24 (m, 1H), 2.27 (t, J = 8.0 Hz, 2H), 2.59 (dd, J = 12.0, 6.0 Hz, 1H), 3.53 (s, 3H), 3.79 (s, 3H), 3.83 (s, 3H), 3.87 (s, 3H), 4.20–4.28 (m, 4H), 4.32–4.38 (m, 1H), 6.77 (s, 1H) 7.03 (d, J = 7.5 Hz, 1H), 7.12 (d, J = 7.5 Hz, 1H), 7.14 (s, 1H), 7.33 (t, J = 7.5 Hz, 2H) 7.43 (t, J = 7.5 Hz, 2H), 7.69 (d, J = 7.5 Hz, 1H), 7.73 (d, J = 7.5 Hz, 2H), 7.90 (d, J = 7.5 Hz, 2H), 8.58 (d, J = 5.5 Hz, 1H); ^{13}C and DEPTQ (^{13}C) NMR (101 MHz, DMSO-d_6): δ 26.35 (CH_2), 29.11 (CH_2), 31.44 (CH_2), 35.63 (CH_2), 46.53 (CH), 51.11 (CH), 53.24 (CH), 55.73 (CH_3), 55.94 (CH_3), 60.59 (CH_3), 60.76 (CH_3), 65.57 (CH_2), 107.63 (CH), 112.04 (CH), 120.02 (2 CH), 125.21(CH), 125.23 (C), 125.33 (CH), 127.01 (2 CH), 127.56 (2 CH), 130.27 (CH), 134.13 (C), 134.33 (CH), 135.10 (C), 140.60 (C), 140.62 (2 C), 143.72 (C), 143.73 (C) 150.35 (C), 150.71 (C), 152.84 (C), 156.05 (CO–NH–OR), 163.43 (C), 170.57 (CO–OH), 173.53 (CO–NHR), 177.90 (CO); LC–MS *m/z*: 709 ($M+H^+$), RT = 9.59 min.

*[Fmoc–Asp(Amonafide)–OH] (**3c**)* Compound **3c** was obtained as brownish solid with 93 % yield from 4c or with 82 % yield from 4i. ^{1}H NMR: (400 MHz, DMSO-d_6): 2.84 (dd, J = 16.0, 6.0 Hz, 1H), 2.90 (s, 3H), 2.91 (s, 3H), 3.01 (dd, J = 16.0, 6.0 Hz, 1H), 3.44–3.48 (br. q, 2H), 4.22 (t, 7.0 Hz, 1H), 4.29–4.31 (m, 2H), 4.39 (t, J = 5.0 Hz, 2H), 4.56 (m, 1H), 7.29 (t, J = 7.5, 1.5 Hz, 2H), 7.39 (t, J = 7.5 Hz, 2H), 7.71 (dd, J = 8.0, 1.0 Hz, 2H), 7.81–7.86 (m, 2H), 7.88 (d, J = 7.0 Hz, 2H), 8.38–8.41 (m, 2H), 8.69 (d, J = 2.0 Hz, 1H), 8.77 (d, J = 2.0 Hz, 1H), 9.36 (s, 1H), 10.71 (s, 1H); DEPTQ (^{13}C) NMR (101 MHz, DMSO-d_6): δ 35.07 (CH_2), 38.22 (CH_2), 42.64 (2 CH_3), 46.48 (CH), 50.30 (CH), 54.73 (CH_2), 65.66 (CH_2), 120.01 (2 CH), 120.85 (CH), 121.87 (C), 122.65 (C), 123.79 (CH), 124.03 (C), 125.11(CH), 125.14 (CH), 126.96 (2 CH), 127.52 (3 CH), 128.99 (CH), 131.99 (C), 133.84 (CH), 137.77 (C), 140.59 (2 C), 143.64 (C), 143.68 (C), 155.81 (CO–NH–OR), 163.68 (CO–NR–CO), 163.94 (CO-NR-CO), 168.91 (CO–OH), 172.84 (CO–NHR); HRMS: ESI–MS *m/z* calcd: 643.217, found: 643.210 ($M+Na^+$), calcd: 659.191 ($M+K^+$), found: 659.182 ($M+K^+$); LC–MS *m/z*: 621 ($M+H^+$), RT = 8.62 min.

*[Fmoc–Glu(Amonafide)–OH] (**3d**)* Compound **3d** was obtained as brownish solid with 88 % yield from **4d** or with 74 % yield from 4j. ^{1}H NMR: (400 MHz, DMSO-d_6): δ 1.89–2.00 (m, 1H), 2.14–2.23 (m, 1H), 2.58 (t, 7.5 Hz, 2H), 2.91 (s, 3H), 2.92 (s, 3H), 3.42–3.50 (m, 2H), 4.06–4.12 (m, 1H), 4.21 (d, J = 7.0 Hz, 1H), 4.26–4.32 (m, 2H), 4.38 (t, 5.0 Hz, 2H), 7.33 (t, J = 7.5, 2H) 7.41 (t, J = 7.5 Hz, 2H), 7.73 (d, J = 7.5 Hz, 2H), 7.77 (d, J = 7.5 Hz, 1H), 7.82 (t, J = 7.5 Hz, 1H), 7.89 (d, J = 7.5 Hz, 2H), 8.36–8.40 (m, 2H), 8.67 (d, 2 Hz, 1H), 8.76 (d, 2 Hz, 1H), 9.36 (s, 1H), 10.62 (s, 1H); ^{13}C and DEPTQ (^{13}C) NMR (101 MHz, DMSO-d_6): δ 26.19 (CH_2), 32.74 (CH_2), 35.06 (CH_2), 42.66 (2 CH_3), 46.53 (CH), 53.22 (CH), 54.82 (CH_2), 64.83 (CH_2), 65.59 (CH_2), 120.01 (CH), 120.03 (CH), 120.74 (CH), 121.93 (C), 122.61 (C), 123.83 (CH), 123.99 (C), 125.17(CH), 125.20 (CH), 126.98 (2 CH), 127.49 (CH), 127.55 (2 CH), 128.92 (CH), 130.00 (C), 133.81 (CH), 137.92 (C), 140.60 (C), 140.62 (C), 143.68 (C), 143.73 (C), 156.13 (CO–NH–OR), 163.69 (CO–NR–CO), 163.94 (CO–NR–CO), 171.14 (CO–OH), 173.59 (CO–NHR); LC–MS *m/z*: 635 ($M+H^+$), RT = 8.73 min.

*[Fmoc–Asp(Cytarabine)–OH] (**3e**)* Compound **3e** was obtained as white solid with 94 % yield from 4e or with 45 % yield from 4 k. ^{1}H NMR: (400 MHz, DMSO-d_6): δ 2.78 (dd, 15, 6 Hz), 2.95 (dd, 15, 6 Hz), 3.62 (d, J = 5.4 Hz, 2H), 3.82–3.85 (m, 1H), 3.93 (t, J = 3.5 Hz, 1H), 4.06–4.08 (m, 1H), 4.20–4.30 (m, 3H), 4.40–4.47 (m, 1H), 4.73–5.85 (br s, 3 [OH]), 6.06 (d, 4.0 Hz, 1H), 7.16 (d, J = 7.5 Hz, 1H), 7.32 (t, J = 7.5 Hz, 2H), 7.41 (t, J = 7.5 Hz, 2H), 7.71 (d, J = 7.5 Hz, 2H), 7.76 (d, J = 7.5 Hz, 1H), 7.89 (d, J = 7.5 Hz, 2H), 8.08 (d, J = 7.5 Hz, 1H), 10.93 (s, 1H); DEPTQ (^{13}C) NMR (400 MHz, DMSO-d_6): δ 38.09 (CH_2), 46.46 (CH), 49.86 (CH), 60.97 (CH_2), 65.60 (CH_2), 74.47 (CH), 76.01 (CH), 85.69 (CH), 86.92 (CH), 94.23 (CH), 120.01 (2 CH), 125.14 (CH), 125.16 (CH), 126.97 (2 CH), 127.53 (2 CH), 140.59 (2 C), 143.67 (2 C), 146.72 (CH), 154.29 (CO–(NR_2)$_2$), 155.72 (CO–NHR–OR), 161.92 (C), 170.53 (CO–OR), 172.69 (CO–NHR); LC–MS *m/z*: 581 ($M+H^+$), RT = 8.79 min.

*[Fmoc–Glu(Cytarabine)–OH] (**3f**)* Compound **3f** was obtained as white solid with 93 % yield from 4f or with 37 % yield from 4 l. ^{1}H NMR: (400 MHz, DMSO-d_6): δ 1.77–1.87 (m, 1H), 2.02–2.10 (m, 1H), 2.51–2.55 (m, 2H), 3.62 (d, J = 5.0 Hz, 2H), 3.81–3.85 (m, 1H), 3.93 (t, J = 3.5 Hz, 1H), 4.06 (dd, J = 4.0, 2.5 Hz, 1H), 4.21–4.30 (m, 3H), 4.36–5.00 (br s, 3 [OH]), 6.06 (d, 4.0 Hz, 1H), 7.19 (d, J = 7.5 Hz, 1H), 7.34 (tt, J = 7.5, 1.5 Hz, 2H), 7.42 (t, J = 7.5 Hz, 2H), 7.68 (d, J = 7.5 Hz, 1H), 7.73 (d, J = 7.5 Hz, 2H), 7.90 (d, J = 7.5 Hz, 2H), 8.07 (d,

J = 7.5 Hz, 1H), 10.98 (s, 1H); ^{13}C and DEPTQ (^{13}C) NMR (400 MHz, DMSO-d_6): δ 25.66 (CH_2), 32.81 (CH_2), 46.52 (CH), 52.98 (CH), 60.90 (CH_2), 65.61 (CH_2), 74.48 (CH), 76.00 (CH), 85.67 (CH), 86.88 (CH), 94.21 (CH), 120.02 (CH), 120.03 (CH), 125.16 (CH), 125.19 (CH), 126.99 (2 CH), 127.54 (2 CH), 140.60 (C), 140.62 (C), 143.69 (C), 143.71 (C), 146.65 (CH), 154.31 (CO-$(NR_2)_2$), 156.06 (CO-NHR-OR), 161.96 (C), 172.88 (CO-OR), 173.48 (CO-NHR); LC–MS *m/z*: 595 ($M+H^+$), RT = 8.83 min.

Synthetic Procedure of ***5***

[Fmoc–Lys(CPT)–OH] (**5**): Fmoc–Lys(Boc) (234 mg, 0.5 mmol) was treated with 90 % TFA in DCM (10 mL). TLC analysis (5 % MeOH in EtOAc) indicated the completion of the reaction after 90 min. The solvent was removed by a nitrogen flow and the crude was precipitated from ether to provide pale orange oil, which was dissolved in DMF. Addition of DIPA (6 eq.) turned the clear solution into a suspension, which was treated dropwise with a dioxane solution of *para*-nitrophenyl chloroformate. The yellow slurry solution was stirred at rt for 4 h. The solvents were removed under reduced pressure. Precipitation from ether resulted in a brown-yellow powder, which was purified by semi-prep. HPLC, affording brown powder in 83 % yield; Rf: 0.70 (25 %MeOH/EtOAc); LC–MS: RT = 9.88 min; ^{1}H NMR (400 MHz, DMSO-d_6): δ 0.92 (t, J = 10.4 Hz, 2H), 1.35 (m, 2H), 1.49 (m, 2H), 1.62 (m, 2H), 2.1 (m, 2H), 2.88 (m, 2H), 4.2 (m, 4H), 5.30 (s, 2H), 5.45 (s, 2H), 7.04 (s, 1H), 7.29 (t, J = 7.3 Hz, 2H), 7.38 (t, J = 7.3 Hz, 2H), 7.52 (d, J = 8.3 Hz, 1H), 7.68 (m, 3H), 7.77 (t, J = 6.2 Hz, 1H), 7.85 (m, 3H), 8.11 (d, J = 8.3 Hz, 1H), 8.18 (d, J = 8.3 Hz, 1H), 8.68 (s, 1H); HRMS: ESI–MS *m/z* calcd:765.254, found: 765.258 ($M+Na^+$), calcd: 781.228, 781.238 ($M+K^+$).

Synthetic Procedure of ***7***

*[RGD-Lys(CPT)-NGR] (**7**)* 2-Chlorotrityl chloride resin with loading capacity of 1.12 mmol/g was placed in a reactor and suspended in DCM under nitrogen atmosphere. A mixture of Fmoc–Asp(OtBu)–OH (2 eq.) and DIPA (8 eq.) in DCM was added. The resin loading reaction was allowed to proceed for 4 h and subsequently the resin was capped by an addition of 0.5 mL of methanol. The Fmoc protecting group was removed with 20 % piperidine/DMF (3 × 7 min) and then a linear SPPS was applied using standard Fmoc procedures. All the couplings were performed in DMF mixtures of Fmoc AA (2 eq.), HATU (2 eq.), and DIPA (6 eq.). Each coupling cycle lasted for 2–3 h. The completion of each coupling reaction or Fmoc removal was monitored by the ninhydrin test. Finally, the Fmoc protecting group was removed from the N-terminal and then the resin was thoroughly washed and dried, and the crude product was cleaved from it by a TFA cocktail [TFA/H_2O/phenol/TIPS (90:5:3:2)], 3 h, rt. The crude was purified by semi-prep HPLC and clean fractions were lyophilized resulting conjugate 7 as yellow powder. LC–MS *m/z*: 1176 ($M+H^+$), RT = 7.79 min, purity >95 %; HRMS: ESI–MS *m/z* calcd: 1176.519, found: 1176.526 ($M+H^+$).

General Procedure for the Synthesis of Cyclic c(RGDf-AA) Drug Conjugates ***8a–d***

2-Chlorotrityl chloride resin with loading capacity of 1.12 mmol/g was placed in a reactor and suspended in DCM under nitrogen atmosphere. A mixture of Fmoc–Asp–OAll (2 eq.) and DIPA (8 eq.) in DCM was added. The resin loading reaction was allowed to proceed for 4 h and subsequently the resin was capped by an addition of 0.5 mL of methanol. The Fmoc protecting group was removed with 20 % piperidine/DMF (10 min × 3) and then a linear SPPS was applied using standard Fmoc procedures. All the couplings were performed in DMF mixtures of Fmoc AA (2 eq.), HATU (2 eq.), and DIPA (6 eq.). Each coupling cycle lasted for 2–3 h. The completion of each coupling reaction or Fmoc removal was monitored by the ninhydrin test. After the coupling of the last AA, the C-terminal allyl ester was removed by exposing the peptidyl resin to a mixture of $Pd(PPh_3)_4$ (0.3 eq.) and DMBA (6 eq.) in DCM for 4 h, after which the resin was thoroughly washed with 0.5 M diethyldithiocarbamic acid sodium salt—DMF solution. Finally, the Fmoc protecting group was removed from the N-terminal and the cyclization reaction was performed by adding a mixture of PyBop (10 eq.), HOBt (10 eq.), DIPA (20 eq.) in NMP and shaking gently for 5 h. After the resin was thoroughly washed and dried, the crude product was cleaved from the resin by a TFA cocktail [TFA/H_2O/Phenol/TIPS (90:5:3:2)], 3 h, rt. The crude was purified by semi-prep HPLC and clean fractions were lyophilized to result the peptide-drug conjugates as crystalline powders.

*[c(RGDfS)-CLB] (**8a**)* Compound **8a** was obtained as pale yellow solid, 62 % yield. LC–MS *m/z*: 848 ($M+H^+$), RT = 9.11 min, purity >95 %; HRMS: ESI–MS *m/z* calcd: 848.327, found: 848.320 (M+H).

*[c(RGDfK)-CPT] (**8b**)* Compound **8b** was obtained as yellow solid, 53 % yield. LC–MS *m/z*: 978 ($M+H^+$), RT = 8.71 min, purity >95 %; HRMS: ESI–MS *m/z* calcd: HRMS: ESI–MS *m/z* calcd: 978.411 found: 978.411 (M+H), calcd: 1000.393, found: 1000.388 (M+Na).

*[c(RGDfE)-Deacetyl Colchicine] (**8c**)* Compound **8c** was obtained as pale yellow solid, 49 % yield. LC–MS *m/z*: 944 ($M+H^+$), RT = 8.41 min, purity >95 %; HRMS: ESI–MS *m/z* calcd: 944.415, found: 944.415 (MH^+).

*[c(RGDfE)-Amonafide] (**8d**)* Compound **8d** was obtained as orange solid, 65 % yield. LC–MS *m/z*: 870 ($M+H^+$), RT = 7.77 min, purity 95 %; HRMS: ESI–MS *m/z* calcd: 870.3898, found: 870.3892 (M+H).

Cytotoxicity Tests

The cytotoxicity of the compounds was determined by measuring the mitochondrial enzymatic activity, using a commercial XTT assay kit. All samples contained DMSO at final concentration <0.05 %.

Cells were cultured in micro wells in a concentration of 2–4 × 10^4 cells/well and allowed to adhere during first 24 h incubation period. At the end of the first 24 h incubation period the cells were washed, given a fresh medium containing different concentrations of the tested substances and subsequently incubated for additional 6 h. At the end of the incubation period with the substances, the medium was removed, all the wells were washed with PBS, given with fresh medium and finally incubated for a second 24 h period. At the end of the second 24 h incubation period the cells were washed again and given a fresh medium containing the XTT reagent after which the cells were re-incubated for 2–4 h. During that time the absorbencies in the wells were measured with a TECAN Infinite M200 ELISA reader at both 480 and 680 nm—the last is the background absorbance. The difference between these measurements was used for calculating the % of Growth Inhibition (GI) in test wells compared to the cells that were exposed only to the medium with 0.05 % DMSO. All the tests were done in tetra-plicate.

Direct Immunofluorescence Assay and Flow Cytometry

For measuring the level of $\alpha_v\beta_3$ integrin expression the cells were washed and then scraped from the culture flacks. For each cell line two separate samples of 10^6 cells were suspended in 200 µL of PBS and incubated in 4 °C—one sample was incubated together with 20 µL pre-diluted mouse 23C6 monoclonal antibody (which is anti-human CD51/CD61) conjugated with R-phycoerythrin (PE) (BD Bioscience), the second sample was free of labeling agent and served as control. During the incubation period the cells were gently shacked every 15 min. After centrifuging and then washing couple of times with PBS, the cells were resuspended in 400 µL of PBS and analyzed using a cell analyzer (Becton Dickson FACSCalibur) equipped with an argon-ion laser (15 W) at 488 nm with a 530/30 DF filter. For each sample ~10^4 cells were analyzed. FlowJo software was used to analyze the data.

Acknowledgments The authors thank Mrs. Cherna Moskowitz for generous stipend to Y.G. Financial support was provided by Ariel University Internal Research and Development Program.

Compliance with Ethical Standards

Conflict of Interest The authors declare that they have no conflict of interest.

Ethical approval This article does not contain any studies with human participants or animals performed by any of the authors.

Informed consent Informed consent was obtained from all individual participants included in the study.

References

Arap W, Pasqualini R, Ruoslahti E (1998) Cancer treatment by targeted drug delivery to tumor vasculature in a mouse model. Science 279:377–380. doi:10.1126/science.279.5349.377

Bagnato JD, Eilers AL, Horton RA, Grissom CB (2004) Synthesis and characterization of a cobalamin–colchicine conjugate as a novel tumor-targeted cytotoxin. J Org Chem 69:8987–8996. doi:10.1021/jo049953w

Bellmann-Sickert K, Beck-Sickinger AG (2010) Peptide drugs to target G protein-coupled receptors. Trends Pharmacol Sci 31:434–441. doi:10.1016/j.tips.2010.06.003

Chen K, Chen X (2011) Integrin targeted delivery of chemotherapeutics. Theranostics 1:189–200

Cheng NC, van Zandwijk N, Reid G (2014) Cilengitide inhibits attachment and invasion of malignant pleural mesothelioma cells through antagonism of integrins αvβ3 and αvβ5. PLoS One 9:e90374. doi:10.1371/journal.pone.0090374

Cohen S, Cahan R, Ben-Dov E, Nisnevitch M, Zaritsky A, Firer MA (2007) Specific targeting to murine myeloma cells of Cyt1Aa toxin from bacillus thuringiensis subspecies israelensis. J Biol Chem 282:28301–28308. doi:10.1074/jbc.M703567200

Colombo G et al (2002) Structure-activity relationships of linear and cyclic peptides containing the NGR tumor-homing motif. J Biol Chem 277:47891–47897. doi:10.1074/jbc.M207500200

Corti A, Curnis F (2011) Isoaspartate-dependent molecular switches for integrin–ligand recognition. J Cell Sci 124:515–522. doi:10.1242/jcs.077172

Corti A, Curnis F, Arap W, Pasqualini R (2008) The neovasculature homing motif NGR: more than meets the eye. Blood 112:2628–2635. doi:10.1182/blood-2008-04-150862

Curnis F, Longhi R, Crippa L, Cattaneo A, Dondossola E, Bachi A, Corti A (2006) Spontaneous formation of L-isoaspartate and gain of function in fibronectin. J Biol Chem 281:36466–36476. doi:10.1074/jbc.M604812200

Dai X, Su Z, Liu JO (2000) An improved synthesis of a selective αvβ3-integrin antagonist cyclo(-RGDfK-). Tetrahedron Lett 41:6295–6298. doi:10.1016/S0040-4039(00)01060-1

Dal Pozzo A et al (2010) Novel tumor-targeted RGD peptide–camptothecin conjugates: synthesis and biological evaluation. Bioorg Med Chem 18:64–72. doi:10.1016/j.bmc.2009.11.019

Danhier F, Breton AL, Préat V (2012) RGD-based strategies to target alpha(v) beta(3) integrin in cancer therapy and diagnosis. Mol Pharm 9:2961–2973. doi:10.1021/mp3002733

Firer M, Gellerman G (2012) Targeted drug delivery for cancer therapy: the other side of antibodies. J Hematol Oncol 5:70

Friligou I et al (2013) Divergent and convergent synthesis of polymannosylated dibranched antigenic peptide of the immunodominant epitope MBP(83–99). Bioorg Med Chem 21:6718–6725. doi:10.1016/j.bmc.2013.08.008

Gellerman G, Elgavi A, Salitra Y, Kramer M (2001) Facile synthesis of orthogonally protected amino acid building blocks for combinatorial N-backbone cyclic peptide chemistry. J Pept Res 57:277–291. doi:10.1046/j.1397-002x.2000.0780.x

Gilad Y, Firer MA, Rozovsky A, Ragozin E, Redko B, Albeck A, Gellerman G (2014) "Switch off/switch on" regulation of drug cytotoxicity by conjugation to a cell targeting peptide. Eur J Med Chem 85:139–146. doi:10.1016/j.ejmech.2014.07.073

Goldshaid L et al (2010) Novel design principles enable specific targeting of imaging and therapeutic agents to necrotic domains in breast tumors. Breast Cancer Res 12:R29

Goodman SL, Picard M (2012) Integrins as therapeutic targets. Trends Pharmacol Sci 33:405–412. doi:10.1016/j.tips.2012.04.002

Gurrath M, Muller G, Kessler H, Aumailley M, Timpl R (1992) Conformation/activity studies of rationally designed potent anti-adhesive RGD peptides. Eur J Biochem 210:911–921. doi:10.1111/j.1432-1033.1992.tb17495.x

Haubner R, Finsinger D, Kessler H (1997) Stereoisomeric peptide libraries and peptidomimetics for designing selective inhibitors of the αvβ3 integrin for a new cancer therapy. Angew Chem Int Ed 36:1374–1389. doi:10.1002/anie.199713741

Kriek NMAJ, Filippov DV, van den Elst H, Meeuwenoord NJ, Tesser GI, van Boom JH, van der Marel GA (2003) Stepwise solid phase synthesis of uridylylated viral genome-linked peptides using uridylylated amino acid building blocks. Tetrahedron 59:1589–1597. doi:10.1016/S0040-4020(03)00042-5

Lafrenie RM, Gallo S, Podor TJ, Buchanan MR, Orr FW (1994) The relative roles of vitronectin receptor, E-selectin and α4β1 in cancer cell adhesion to interleukin-1-treated endothelial cells. Eur J Cancer 30:2151–2158. doi:10.1016/0959-8049(94)00354-8

Majumdar S, Siahaan TJ (2012) Peptide-mediated targeted drug delivery. Med Res Rev 32:637–658. doi:10.1002/med.20225

Manfredini S et al (2000) Peptide T-araC conjugates: solid-phase synthesis and biological activity of N4-(acylpeptidyl)-araC. Bioorg Med Chem 8:539–547. doi:10.1016/S0968-0896(99)00317-X

Pasqualini R et al (2000) Aminopeptidase N is a receptor for tumor-homing peptides and a target for inhibiting angiogenesis. Cancer Res 60:722–727

Plow EF, Haas TA, Zhang L, Loftus J, Smith JW (2000) Ligand binding to integrins. J Biol Chem 275:21785–21788. doi:10.1074/jbc.R000003200

Reissner KJ, Aswad DW (2003) Deamidation and isoaspartate formation in proteins: unwanted alterations or surreptitious signals? Cell Mol Life Sci 60:1281–1295. doi:10.1007/s00018-003-2287-5

Robinson NE, Robinson ZW, Robinson BR, Robinson AL, Robinson JA, Robinson ML, Robinson AB (2004) Structure-dependent nonenzymatic deamidation of glutaminyl and asparaginyl pentapeptides. J Pept Res 63:426–436. doi:10.1111/j.1399-3011.2004.00151.x

Ruoslahti E (1996) RGD and other recognition sequences for integrins. Annu Rev Cell Dev Biol 12:697–715. doi:10.1146/annurev.cellbio.12.1.697

Ruoslahti E (2002) Specialization of tumour vasculature. Nat Rev Cancer 2:83–90

Shabbir SH, Eisenberg JL, Mrksich M (2010) An inhibitor of a cell adhesion receptor stimulates cell migration. Angew Chem Int Ed 49:7706–7709. doi:10.1002/anie.201002699

Soudy R, Ahmed S, Kaur K (2012) NGR Peptide ligands for targeting CD13/APN identified through peptide array screening resemble fibronectin sequences. ACS Comb Sci 14:590–599. doi:10.1021/co300055s

van Hensbergen Y et al (2002) A doxorubicin-CNGRC-peptide conjugate with prodrug properties. Biochem Pharmacol 63:897–908. doi:10.1016/S0006-2952(01)00928-5

Vig BS, Huttunen KM, Laine K, Rautio J (2013) Amino acids as promoieties in prodrug design and development. Adv Drug Deliv Rev 65:1370–1385. doi:10.1016/j.addr.2012.10.001